EXPERIMENTAL INVESTIGATION OF THE PRESSURE DROP PERFORMANCE AND THE CAVITATION OF A PLUNGER VALVE

A Thesis submitted to
the Graduate School of Engineering and Sciences of
İzmir Institute of Technology
in Partial Fulfillment of the Requirements for the Degree of

MASTER OF SCIENCE

in Mechanical Engineering

by
Emre AYDENİZ

December 2020
İZMİR

ACKNOWLEDGMENTS

Firstly, I would like to thank my supervisor Assoc. Prof. Dr. Ünver ÖZKOL for his supportsandadvicesduringmystudiesandresearches.Iamalsogratefulthathegaveme opportunity by taking part in his project that positively affected my perspective and studies.

I would like to thank Doğuş Vana company for giving us a job opportunity with this TUBITAK project.

I would like to thank to Research and Development manager of the Doğuş Vana Alaattin YILDIRIM and also I would like to thank my school and also my colleague Bedia AKBULUT.

I would very much like to thank my parents: Semra AYDENİZ and Ahmet AYDENİZ for their endless support throughout my life.

And finally, I would like to thank Electrical & Electronics Engineer Emre ÇANCIOĞLU, Mechatronics Engineer Süleyman GÜRCAN and Sezer GÜLER, who provided technical support for me in test setup in this project.

ABSTRACT

EXPERIMENTAL INVESTIGATION OF THE PRESSURE DROP PERFORMANCE AND THE CAVITATION OF A PLUNGER VALVE

This thesis, realized within the scope of a TUBITAK project of DOĞUŞ VANA A.Ş, is aimed to characterize the pressure drop and cavitation performance of plunger valve with various cavitation lattices in different opening ratios. Pressure drop performance and cavitation studies have been examined experimentally. Loss coefficients and flow coefficients were used to examine the pressure drop performance of four different types of cavitation lattices. According to the results of this experimental study, it was observed that the loss coefficient is almost independent of Reynolds number except for $Re < 4x10^{5.}$

Cavitation creates vibration and noise in high-frequency ranges. Therefore, cavitation detection was examined in the high-frequency range of 5 kHz to 18 kHz and was performed using an accelerometer. Fourier Transform (FT) and Power Spectrum Density (PSD) were used to measure the energy levels of vibrations. Cavitation limits (incipient and critical cavitation) were detected by comparing PSD levels and cavitation indexes at different aperture ratios for all lattices. As a result, the safe cavitation range for the valve was determined by comparing the cavitation indexes according to the valve opening ratio.

A new cavitation index estimation study was performed for the new diameter and upstream pressure values with the effect of size scaling and pressure scaling.

ÖZET

İĞNELİ VANALARDA BASINÇ DÜŞÜMÜ PERFORMANSININ VE KAVİTASYONUN DENEYSEL İNCELENMESİ

TÜBİTAK projesi kapsamında gerçekleştirilen bu tezin amacı, farklı açıklık oranlarında çeşitli kavitasyon kafesleri ile iğneli vananın basınç düşüş performansını ve kavitasyonunu karakterize etmektir. Bu çalışma DOĞUŞ VANA firması ile yapılmıştır. Basınç düşüş performansı ve kavitasyon çalışmaları deneysel olarak incelenmiştir. Dört farklı kafes türünün basınç düşüş performansı incelemek için kayıp katsayıları ve akış katsayıları kullanılmıştır. Bu deneysel çalışmanın sonuçlarına göre, kayıp katsayısının Re $<4x10^5$ dışında Reynolds sayısından neredeyse bağımsız olduğu görülmüştür.Kavitasyon, yüksek frekans aralıklarında titreşim sesleri oluşturur. Bu nedenle, 5 kHz ile 18 kHz arasındaki yüksek frekans aralıklarında kavitasyon tespiti incelendi ve ivmeölçer kullanılarak gerçekleştirildi. Fourier Dönüşümü (FT) ve dB cinsinden Güç Spektrum Yoğunluğu (PSD), titreşimlerin enerji seviyelerini ölçmek için kullanılmıştır. Tüm kafesler için farklı açıklık oranlarında dB ve kavitasyon indeksleri karşılaştırılarak kavitasyon sınırları (başlangıç ve kritik kavitasyon) tespit edildi. Sonuç olarak, vana açıklık oranına göre kavitasyon indeksleri karşılaştırılarak vana için güvenli kavitasyon aralığı belirlendi.

Boyut ölçeklendirmesi ve basınç ölçeklendirmesinin etkisiyle yeni çap ve yukarı akış basınç değerleri için yeni bir kavitasyon indeksi tahmin çalışması yapıldı.

TABLE OF CONTENTS

LIST OF FIGURES

Figure **Page**

Figure **Page**

Figure **Page**

Figure **Page**

LIST OF TABLES

Table **Page**

LIST OF SYMBOLS

SYMBOLS

K	Loss Coefficient
C_v	Flow Coefficient
V	Average Velocity
ΔP	Pressure Difference
Q	Flow Rate
A	Area
σ	Cavitation Index
g	gravitational acceleration
V_{id}	Incipient damage velocity
F_L	Liquid pressure recovery
F_F	Liquid critical pressure ratio
q_{max}	Maximum flow rate
Re	Reynolds number
G_f	Liquid specific gravity
SSE	Size scale effect
PSE	Pressure scale effect
d	Valve diameter
d_R	Reference valve diameter
ρ	density
σ_i	Incipient Cavitation Index
σ_c	Critical Cavitation Index

INDICES

max	maximum
f	fluid
L	length
id	Inc. damage
i	Incipient
c	Critical

CHAPTER 1

INTRODUCTION

Cavitation is the one of the seriously damaging problems that is seen in some hydraulic systems that carries liquid such as valves and pumps where engineers must consider during a design stage. It severely damages hydraulic systems by causing erosion on solid surfaces and occurs when the flow rate is high and the pressure is lower than vapor pressure of the liquid. The negative effects of a cavitating hydraulic system besides the erosion are very noisy operation, high vibrations that may cause disintegration in a long run and the lowered operational life of the system. These negative effects can be avoided careful design strategies.

In this study, flow characteristic and cavitation experiments of Plunger valves with or without a cavitation suppressing device (a.k.a Cavitation lattice) have been done and safe operational limits for designers are established. Experimental work, was aimed to find safe operational limits for a Plunger valve under the cavitation by using vibration level measurement methods. Using various cavitation lattice geometries, cavitation parameters were compared according to the opening ratios and safe cavitation limits were determined. Details will be explained in the following chapters.

1.1. Definition of Cavitation

Cavitation is the formation and collapse of small vapor cavities or bubbles in a liquid. It occurs when a liquid is subjected to drop of pressure lower than the liquid's vapor pressure for some extended time which will cause the formation of vapor bubbles, following a pressure rise which results in a bubble collapse. When this collapse occurs near a solid surface, it creates an unsymmetrical surrounding for the bubble and this creates a micro jet of liquid towards the solid surface due this unsymmetric collapse. This jet is very high speed jet creates an impact on the surface which causes fatigue related erosion from the surface over time.

1.1.1.The physical Phenomenon

Cavitation is the rapid vaporization of a liquid followed by sudden condensation. The process is somewhat similar to the boiling process in which vapor bubbles form when the vapor pressure reaches atmospheric pressure by heating the liquid. The main difference separating cavitation from boiling is pressure and temperature. Cavitation is a phase change process caused by sudden pressure drop under constant temperature, as shown in the Figure 1.1 .(Libera, 2015)

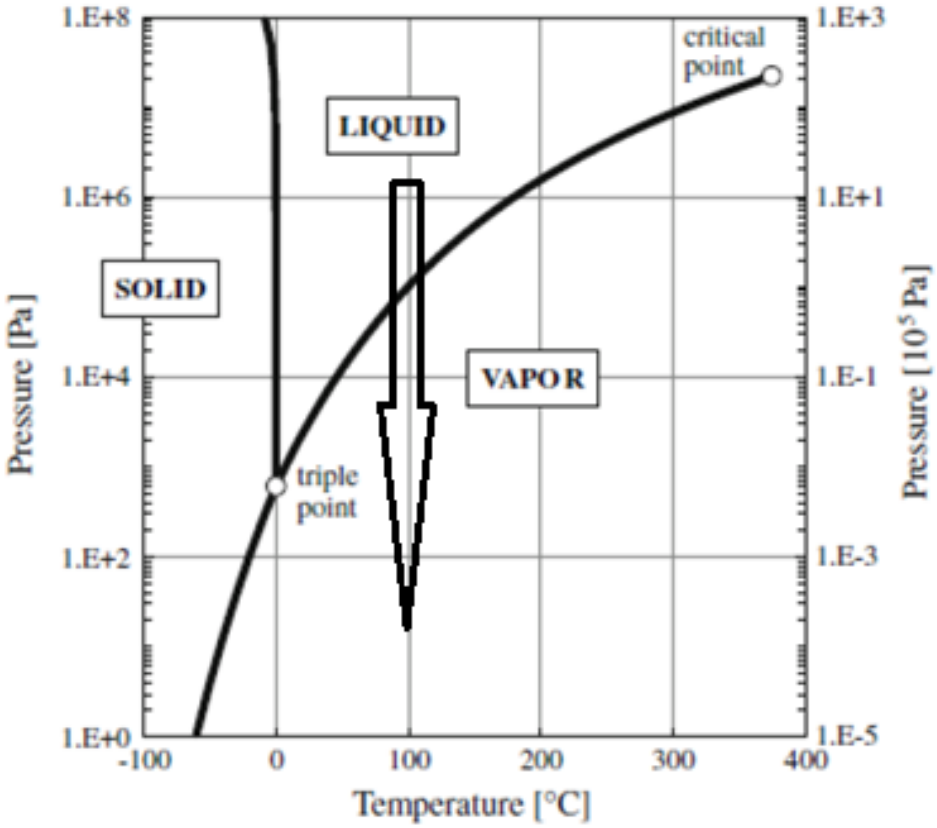

Figure 1.1 Phase diagram of water (Source: .(Libera, 2015))

In high flow rates, where the fluid passes through a narrow or constricted area (such as a Vena Contracta or a valve with a very narrow opening), speed of liquid increases and its pressure drops, according to the Bernoulli equation. If the pressure of the liquid stays lower than the vapor pressure at a given temperature bubbles formed and start to grow by moving in the direction of flow as shown in the Figure 1.2. Collapse of bubbles occurs by rise of pressure and surface tension (Soyama and Hoshino, 2016).

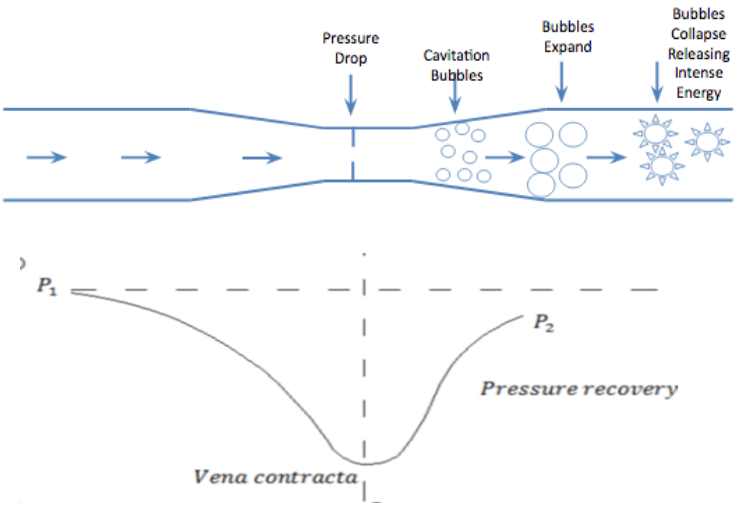

Figure 1.2 Pressure Recovery (Soyama and Hoshino, 2016)

1.1.2 The Effect of Cavitation on Hydrodynamics

There are several useful practices for cavitation as well. High-grade turbulence associated with cavitation can be used to increase mixing, speed up chemical reactions and form the basis of ultrasonic cleaning devices. However, in most hydraulic systems, cavitation has a detrimental effect. Noise, vibration, pressure fluctuations, erosion damage, accelerated corrosion, and loss of efficiency or flow capacity are at least six fundamental problems (J. Paul, 1993).In particular, it can cause serious damage to valves and pumps, which not only reduce their performance but also cause early damage and economical consequences as seen Figure 1.3.

Figure 1.3: Effect of Cavitation on Valve Surface

Apart from the noise and vibrations caused by the condensation of bubbles, they create cavities in the valve body and pipe walls and begin to erode over time (Zhao et al., 2007).There are two mechanisms were proposed that can explain the damage at solid boundaries. The first of these is the high pressure shock wave caused by cavity collapse. It damages the material surface by applying pressure greater than 70 kbar (J. Paul, 1993). As shown in the Figure 1.4, another potential source of damage is the micro jet. When the bubble collapses near the boundary, the pressure distribution around the bubble is asymmetrical due to the boundary effect. As the bubbles collapse, the side of the bubble away from the wall reaches a higher velocity, the bubble collapses inward and a jet is created from the center of the bubble. The jet reaches a very high velocity and when it hits the wall it creates a high and localized impact. These impacts over time fatigue the surface and eventual erosion.

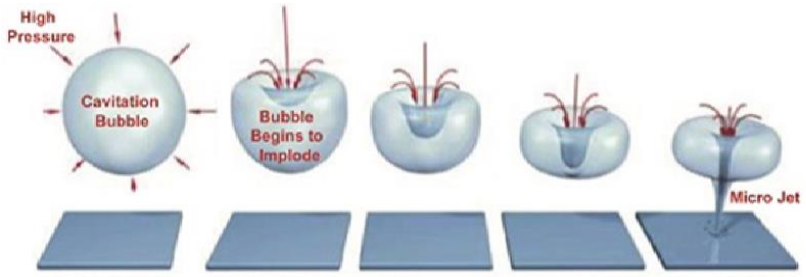

Figure 1.4 : Behavior of bubbles on wall surface

1.1.3 Cavitation Noise and Vibration

Noise and vibrations are generated by the growth and collapse of bubbles caused by cavitation. In particular, the bubble collapse is accompanied by high flow velocity and high fluid pressure in the cavitation bubble region, thereby creating pressure fluctuaitons (Brennen, 2013),(Jablonská, Mahdal, and Kozubková, 2017) and .(Meng et al., 2017)

Some popping noises occur in the initial stages of cavitation. In areas where it is more intense, the hissing (like the sound of gas coming out of the stove) occurs. Some researchers describe this noise as rolling pebbles inside a pipe (J.P.Tullis 1993). This noise can be heard simply because it is louder than the turbulence noise generated.

Some experimental studies were performed to detect this cavitation vibration and noise by spectral analysis. (Samuel Martin et al., 1981)used a microphone sensor

located near to detect the severity of cavitation on a spool valve. In his study, he applied spectral analysis with different cavitation indices and determined in what frequency range cavitation occurred. According to this study, cavitation was shown in the frequency range of 5 kHz and above, and as the cavitation index increased which indicate increase in the severity of cavitation, the minimum frequency values decreased accordingly as shown Figure 1.5.

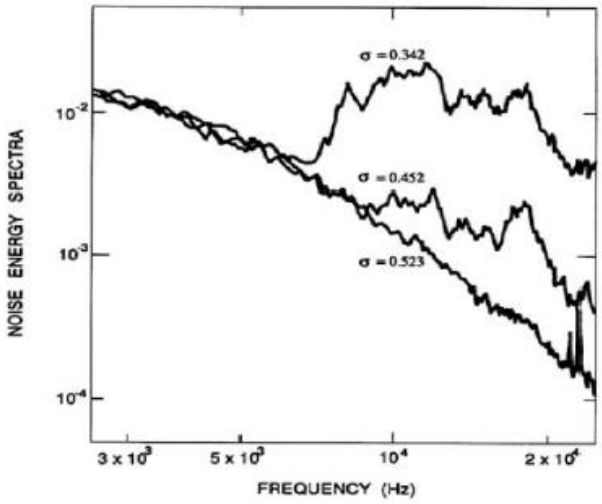

Figure 1.5 Frequency spectrum of the noise at different cavitation index(Source : Samuel Martin et al., 1981)

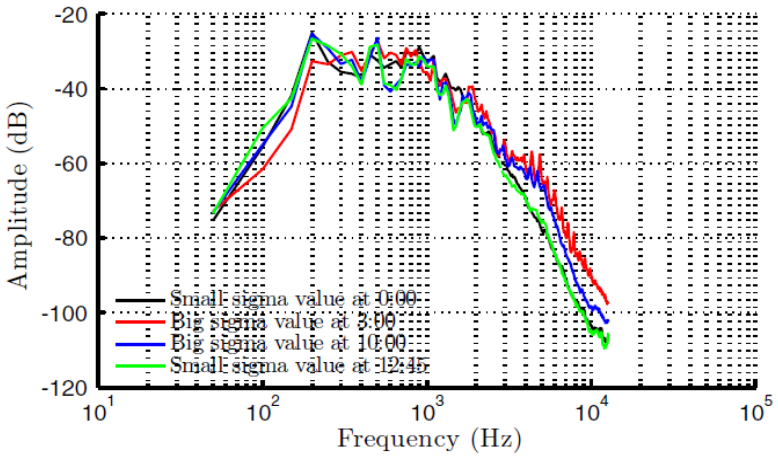

Figure 1.6 Noise spectra from the downstream pipe at different times. (Source: Ulanicki, Picinali, and Janus, 2015)

The pressure reducing valve was examined under the conditions which cavitation occurs by (Ulanicki, Picinali, and Janus, 2015).Vibrations measured at

different time intervals and different cavitation indexes were examined spectrally in this study vibration frequencies varied where the cavitation index was large and small. As shown in Figure 1.6, low cavitation indexes occur at low frequencies, while large cavitation indexes occur in large frequency ranges. Explained this theory that while small bubbles generate high frequency, large bubbles occur at low frequency.

1.2 Valve Characterization

Valves are an essential part of pipeline design. They are used to regulate flow and pressure, protect piping and pumps from overpressure, and help prevent transitions, prevent reverse flow from pumps, remove air, and perform various other functions.

All control valves have an inherent flow characteristic that defines the relationship between valve opening and flow rate under constant pressure conditions. Valve opening refers to the relative position of the valve plug to its closed position against the valve seat.

1.2.1 Flow and Loss Coefficients

The hydraulic characteristics of the valves, the relationship between flow and pressure drop at any valve opening, can be expressed in a number of coefficients. The most common of these coefficients used in engineering are shown in the Equations 1.1 and 1.2.

Pressure drop introduced by valves are formulated ;

$$K = \frac{2 \times \Delta P}{\rho \times V^2} \tag{1.1}$$

The American National Standart Institute (ANSI) has made change to the pressure drop equation and obtained the following flow coefficient;

$$C_V = \frac{Q}{\sqrt{\Delta P}} \tag{1.2}$$

In which V is the average velocity at the inlet to the valve, ρ is the fluid density at the upstream fluid temperature and ΔP is the net pressure drop accros the valve. There is a proportionality between flow coefficient and loss coefficient as shown in Equation 1.5. Therefore, it is possible to calculate the flow coefficient from the pressure coefficient.

$$\Delta P = \frac{Q^2}{C_V{}^2} = \frac{V^2 \times A^2}{C_V{}^2} \tag{1.3}$$

$$K = \frac{2 \times V^2 \times A^2}{C_V{}^2 \times \rho \times V^2} \tag{1.4}$$

$$K = \frac{2 \times A^2}{C_V{}^2 \times \rho} \tag{1.5}$$

1.3 Plunger Valve

The Plunger valve is mainly designed to provide flow and pressure regulation in a pipeline. Regulation is carried out by the shaft crank mechanism moving the piston axially. The plunger is located in a chamber in the middle of the valve. This part is designed to protect the piston from water flow and prevent noises and cavitation damages and allows it to operate without vibration. The components of Plunger valve were shown in Figure 1.7.

As shown in Figure 1.8, the water flow is directed into an annular chamber around the central body of the valve. The cross section of this chamber constantly decreases from entrance to exit. Therefore, the flow velocity increases and the pressure decreases.

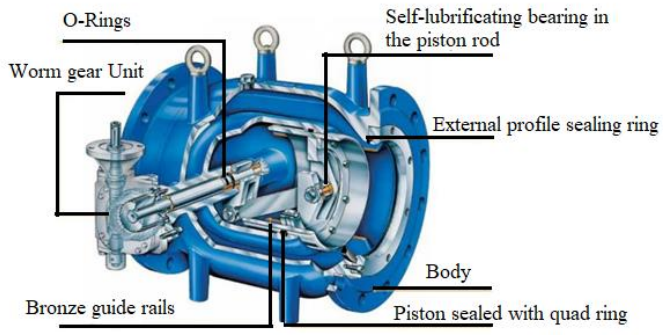

Figure 1.7 Cross-section of Plunger Valve
(Source: Ulanicki, Picinali, and Janus, 2015)

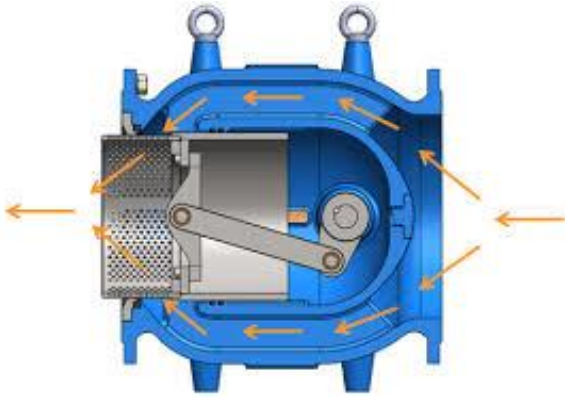

Figure 1.8 Water Flow around the Annular Chamber
(Source: AvTekValves, 2017)

Various methods are used to reduce the damage of cavitation. One of these methods is using a cavitation lattice. Sudden decrease of outlet pressure can be prevented by dividing the flow various paths by means of a cavitation lattice at the outlet of the plunger valve as seen Figure 1.9. This lattice cause pressure drops at through each hole besides the pressure drop caused by the original geometry of the valve itself. This reduces the risk of cavitation by distributing the sudden pressure drop on a larger area. This method also regulates the regime of the flow. There are also some disadvantages. For example, some waste materials (stone, plastic, paper, etc.) may enter between the holes and block some parts of the lattice holes.

There are two types of lattices commonly used. That are slots or holes around the lattice.

Figure 1.9 Orifice Lattice and Slotted lattice
(Source : DVD Valve, 2015)

L.Gianandrea investigated to some cavitation lattice to cavitation index against valve opening ratio. The lattices are compared between each other. LH and SZ model

cavitation lattice represent to orifice and slot type cavitation lattice respectively. LH model cavitation lattice is in safer operational limit compared to other lattices (Libera, 2015).

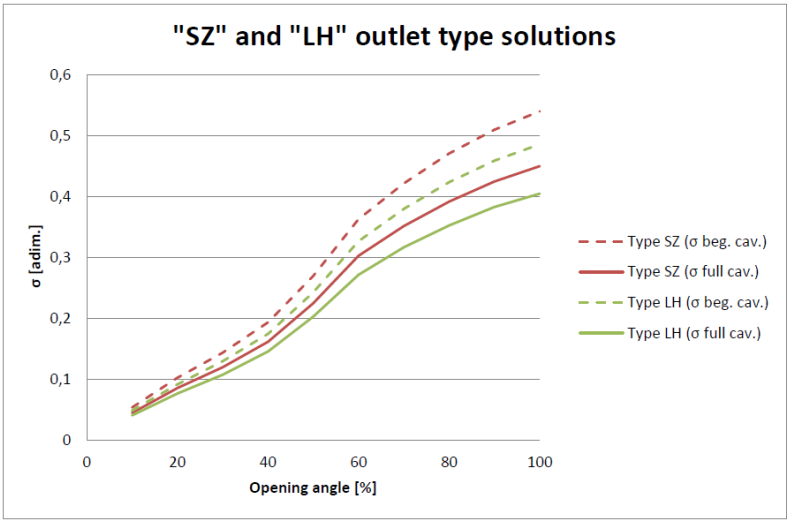

Figure 1.10 LH and SZ Lattices were compared.
(Source: Libera, 2015)

1.4 Motivation

The aim of this thesis is investigated to the pressure drop performance and cavitation limits of the Plunger valve with experimental methods. The plunger valve is aimed to operate within safe cavitation limits. The cavitation lattices were designed in different holes types were mounted on the plunger valve and a comparison was made between cavitation limits.

In addition, it is to detect the cavitation limits in different diameter or pressure conditions with the effect of size and pressure scale without the need to experiment.

CHAPTER 2

CAVITATION PARAMETER AND LIMITS

Cavitation has a very important role in determining the proper working conditions of valve and pipe systems. Cavitation intensity and its effect on hydraulic systems generally vary according to valve type, operating pressure and pipeline installation type. It is important to understand whether there is cavitation on the system and to estimate it to determine the intensity and characteristics of the cavitation. If it is not predictable, it will cause negative effects such as noise, vibration, erosion and performance degradation.

Dimensionless similarity parameters are the best method for determining flow conditions corresponding to a given cavitation intensity. Parameters such as "Euler number (Eu), Reynolds Number (Re), Weber Number (We) and Cavitation Index (sigma)" are important parameters derived from non-dimensional analysis. The Euler number (Eu) is a parameter corresponding to the ratio of the inertial forces to the pressure forces, it also defines the level of energy expended in the valves. Reynolds Number equals to ratio of the inertial forces to viscosity forces. Since it is inverse ratio to viscosity forces when the viscosity forces increase, the effect of Reynolds numbers decreases. However, scale effect that will mentioned later is an important relation to Reynolds Number. The Weber number is the ratio of the inertial forces to the surface tension forces. The research at the literature shows that the effect of the surface tension was little effect at incipient cavitation (Holl, 1960). Cavitation index (sigma) represents the rate of pressure drop obtained from kinetic energy of the pressure drop required for the occurrence of the vapor cavity. It is the most useful for parameters that are mentioned and it is a good indicator for detecting the cavitation (B. Mumford,1985).

2.1 Cavitation Quantification

Various cavitation index definitions have been used for valves, pump and turbine in literature. In this study, the cavitation index (σ) calculated for cavitation in valves according to the ISA (International Society of America,1995) standard was used.

This index is found in proportion to the force that tries to suppress cavitation and the force that causes cavitation. The cavitation parameter sigma can be expressed in equation 2.1.

$$\sigma = \frac{P_1 - P_V}{P_1 - P_2} \tag{2.1}$$

According to equation 2.1 and 2.2, P_1 and P_2 are the mean upstream and downstream absolute pressure of the valve. Pv is absolute vapor pressure of the fluid at inlet temperature. Force acting on cavitation is directly proportional to $\rho*V^2/2*g$ (velocity head) or ΔP_{net} (pressure drop) (J. Paul, 1993).

$$\Delta P_{net} = P_1 - P_2 = \frac{\rho \times V^2}{2 \times g} \tag{2.2}$$

2.2 Detection of Cavitation Limits

Laboratory devices that can detect vibration, noise, pressure fluctuations, pitting and data loss in the system are used to detect cavitation. In order for the determination of cavitation parameters to be sensitive, it is necessary to establish a laboratory that is relatively far from the noise and vibrations caused by the ambient conditions. The accelerometer is the most common sensor used to detect cavitation, as it is easy to use and has precise measurement (Tullis and Colorado, 1976).

A method is used to determine a specific starting point of the cavitation and non-cavitation zone. According to this method, a logarithmic curve is obtained by comparing the data read at the output of the accelerometer with the cavitation index corresponding to m/s^2 or PSD (dB) units.

The cavitation limits must be determined in order to control vibrations and noises caused by cavitation. The main criteria for determining the cavitation limits are as follows;

- Incipient Cavitation
- Critical (or Constant) Cavitation
- Incipient Damage
- Choking Cavitation

2.2.1 Incipient Cavitation

Incipient cavitation is the first point at which cavitation begins, it consists of intermittent light popping noises and can be partially distinguished from the noise generated by the turbulent flow.

The incipient cavitation has no detrimental effect on valve useful life; therefore, it is used only in cases where even a slightest cavitation noise cannot be accepted. For this reason, it is generally not preferred as a design parameter.

2.2.2 Critical Cavitation

The next level is critical, in other words, constant cavitation. At this level, the noise is similar to popcorn popping and is steady. In critical cavitation, there are no situations that will cause a decrease in working life or damage. Usually, the Critical cavitation zone is recommended level of cavitation for situations where “cavitation free operation” in most applications (Distribution, 2015).

The critical cavitation limit is preferred for the operation of the valves because noise and vibrations are not objectionable and would not decrease to working life of Valves.

The Incipient and Critical Cavitation indexes are evaluated by plotting accelerometer outputs (m/s^2 or dB) versus cavitation indexes on log-log coordinates. Example of the plot is shown Figure 2.1

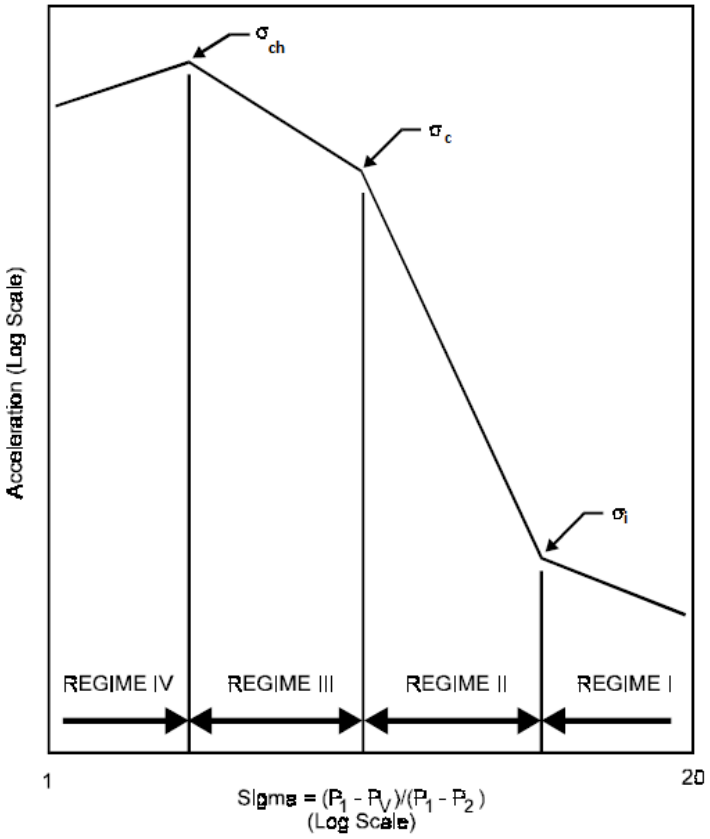

Figure 2.1 Evaluation of Incipient and Critical Cavitation (Source: ISA,1995)

In figure 2.1 the indexes σ_i,σ_c and σ_{ch}respresent:

- σ_i: Incipient Cavitation Index
- σ_c: Critical Cavitation Index
- σ_{ch}: Choking Cavitation Index

According to ISA and modifications define several regime regions of cavitation; Regime I shows that no cavitation. In this regime, there is only a light noise from turbulence. Regime II defines the incipient cavitation region, where small vapor cavities are present. Regime III defines the constant cavitation region, that produce low levels of vibration and Regime IV defines choking cavitation, where peak vibration measurement (Boffi et al., 2019).

2.2.3 Incipient Damage

Incipient damage is defined as the point at which vibration and noise begin to appear damaging, and eroding the solid surface. Determining the incipient damage level

is much more difficult than detecting other cavitation levels and the cavitation characteristic curve detected at incipient and critical cavitation levels cannot be used in this method. The way to detect this point is to measure the pitting rate by using a soft material such as aluminum.

The method used to detect incipient cavitation damage is to plot the maximum cavitation ratio with the velocity of the flow through the pipe. Incipient damage indicates a flow condition on the aluminum surface that causes a pitting rate of 1 $inch^2$ /min (Ball, Tullis, and Stripling, 1975). The cavitation damage test shown in the Figure 2.2. The graph is linear with the logarithmic scale of the pitting rate and velocity. Velocity is a very important factor and small changes to the parameter can greatly affect the damage rate. In equation 2.3 shows that weight loss rating is exponentially proportional to the velocity.

$$\text{Weight Loss} \approx \left(V - V_{id}\right)^n \tag{2.3}$$

Where the V_{id} is velocity at incipient damage and n value has been evaluated experimentally and found to be between 4 and 8(Knapp, R. T., Daily, J. W., and Hammitt, F. G.,1970), (Stripling, T. C, 1975) and (“Sweeney, C. E., 1974).

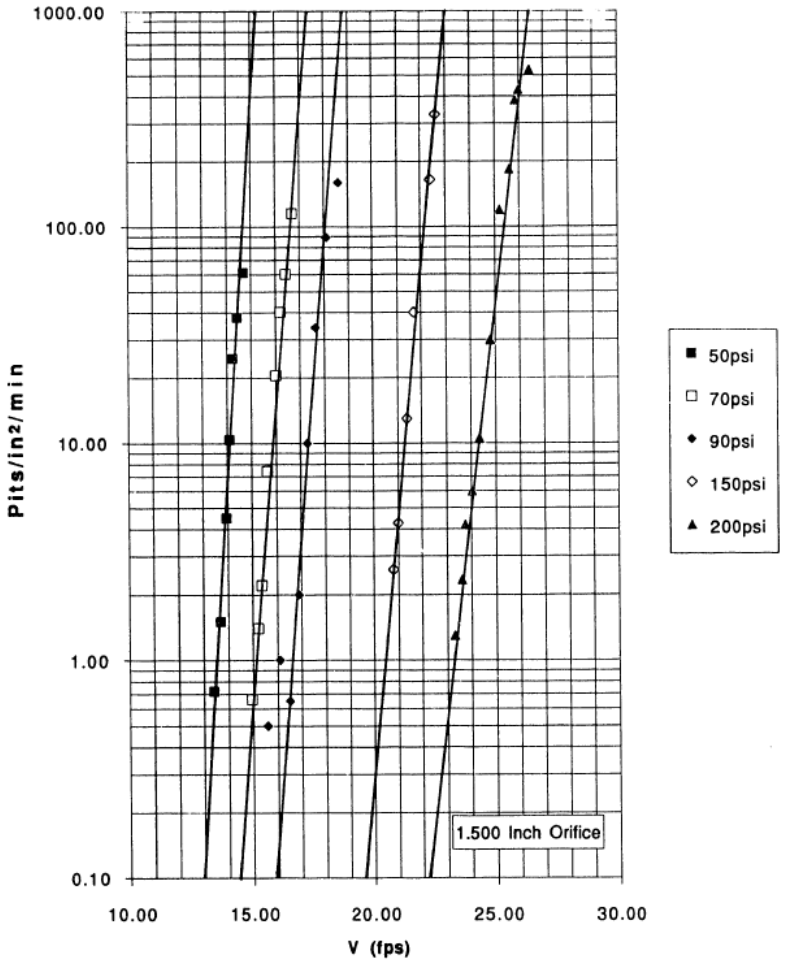

Figure 2.2 Determination of Incipient Damage
(Source: J. Paul, 1993)

2.2.4 Choking Cavitation

Control valves are not preferably operated in the choking cavitation level in long-period applications. Because damage and erosion are severe at this level. When the fluid reaches choked, cavitation creates large volume of vapor cavities until pressure recovery and causes serious damage and erosion as a result of the collapse of those cavities. The choking cavitation can be estimated from the following equations:

$$\sigma_{ch} = \frac{P_1 - P_V}{\Delta P_{choked}} = \frac{P_1 - P_V}{F_L{}^2 (P_1 - F_F P_V)} \tag{2.4}$$

F_L is the liquid pressure recovery factor and F_F is the liquid critical pressure ratio factor.(ISA 1995).

$$F_L = \frac{q_{\max}}{Cv\left[\frac{(P_1 - 0{,}96P_v)}{G_f}\right]^{1/2}} \tag{2.5}$$

$$F_F = \frac{1}{P_v}\left[P_1 - G_f\left(\frac{q_{\max}}{F_L C_v}\right)\right] \tag{2.6}$$

Where the q_{max} is the maximum flow rate of the choked flow, P_1 is the upstream pressure at q_{max} ,G_f is the liquid specific gravity, $C_v$is the valve flow coefficient which is defined at Equation (2.7) and $P_v$is the vapor pressure at upstream temperature.

$$C_v = \frac{q}{\sqrt{\Delta P}} \tag{2.7}$$

When the flow is choked, flow rate through the valve does not any increase in flow rate even if the outlet pressure decreases (pressure difference increase) after the choked flow level. In Figure 2.3, this situation is shown (Ebrahimi et al., 2017).

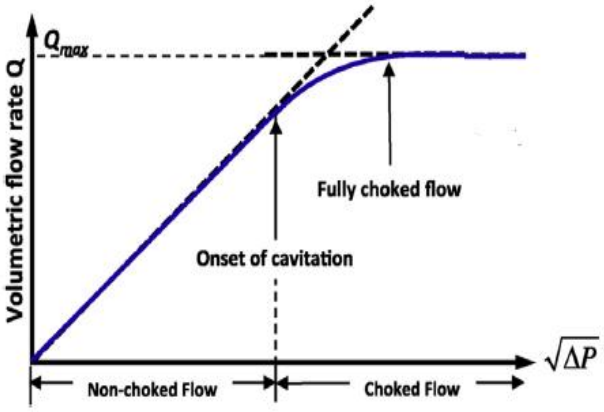

Figure 2.3 Non-choked and Choked Flow
(Source: Ebrahimi et al., 2017)

2.3 Scale Effect

In general, the cavitation tests of the valve are carried out at low pressure and small size diameter due to the limited test conditions. However, sometimes the valve is not so small and the application requires (high pressures) may change. In these conditions, the testing such a large valve is not economical at all. On the other hand,

small diameter valve test data can be converted to be useful for large diameter valves.

Cavitation coefficients depend on different pressure or valve sizes. Some empirical calculations can be used to estimate the cavitation coefficient at large diameters and high pressures. In the past studies, the scale analysis was investigated for the valves by Tullis and his student (Baquero ,1977, Eric S. ,1977, Ted R., 1986). If the cavitation coefficient changes according to the pressure, it is defined as the pressure size effect, if cavitation coefficient changes according to the valve size, it is defined as the valve size effect. The size scale effect and Pressure scale effect were obtained depending on the Reynolds Number (Johnson, 1970),(HAMMITT, 1973).

2.3.1 Size and Pressure Scale Effect

The level of cavitation increase with increasing valve size due to increase. This is because as the size increases, the Reynolds number increases and consequently the turbulence level increases. The size scale effect (SSE) is calculated by Equation (2.8).

$$SSE = \left(\frac{d}{d_R} \right)^Y \tag{2.8}$$

$d_R$is the reference valve diameter and Y is interpreted by:

$$Y = 0,3K^{-0,25} \tag{2.9}$$

Where the K is valve loss coefficient. Equation (2.8) - (2.9) were applied for valves up to 914 mm diameter (Tullis, J. P, 1974).

For valves, the size scale effect is effective for only incipient cavitation (σ_i) and critical cavitation (σ_c). The recommended size scale effect (SSE) equation for (σi) and (σc) are given by Equations (2.11 and 2.12).

$$\sigma_i = SSE(\sigma_{iREF} - 1) + 1 \tag{2.10}$$

$$\sigma_c = SSE(\sigma_{cREF} - 1) + 1 \tag{2.11}$$

The level of cavitation increase with increasing the difference of ($P_1 - P_2$). The pressure scale effect (PSE) is calculated by the following equation.

$$PSE = \left(\frac{P_1 - P_V}{(P_1 - P_V)_R} \right)^X \tag{2.12}$$

The subscript R represents reference absolute pressures of inlet and vapor. The X component that shown Figure (2.4) is a slop of series of approximate straight lines of

the log-log scale plot of incipient, critical, or incipient damage versus (P1-PV). For each opening ratio, different cavitation levels were obtained and a curve was formed. The pressure scale effect (PSE) equation for (σ_i) ,(σ_c) and (σ_{id}) are given by Equations (2.13, 2.14 and 2.15).

$$\sigma_i = PSE(\sigma_{iREF} - 1) + 1 \tag{2.13}$$

$$\sigma_C = PSE(\sigma_{CREF} - 1) + 1 \tag{2.14}$$

$$\sigma_{id} = PSE(\sigma_{idREF} - 1) + 1 \tag{2.15}$$

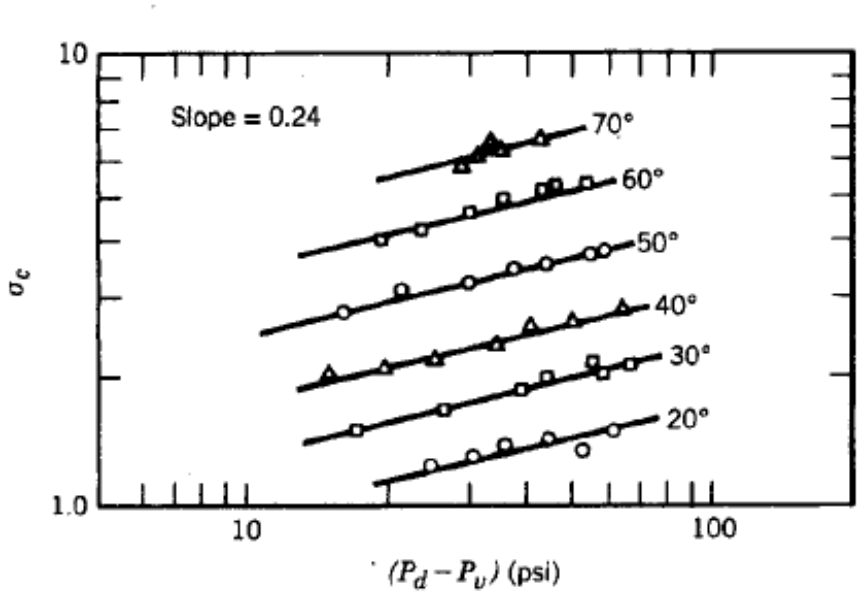

Figure 2.4 PSE for a butterfly valve
(Source: J. Paul, 1993)

Various valves were tested at different cavitation levels to determine the coefficient a shown in Table 2.1. As it is clear from the values in the table, choking cavitation level is not valid for the pressure measurement effect.

Table: 2.1 Pressure Scale Effect for Exponent
(Source: ISA, 1995)

Valve type	Cavitation level	Exponent x
Quarter-turn valves (e.g., ball, butterfly)	Incipient Constant Incipient Damage Choking	0.22 - 0.30 0.22 - 0.30 0.10 - 0.18 0
Segmented ball and eccentric plug	Incipient Constant Incipient Damage Choking	0.30 - 0.40 0.30 - 0.40 N/A 0
Single-stage globe	Incipient Constant Incipient Damage Choking	0.10 - 0.14 0.10 - 0.14 0.08 - 0.11 0
Multi-stage globe	Incipient Constant Incipient Damage Choking	0.00 - 0.10 0.00 - 0.10 N/A 0
Orifice	Incipient Constant Incipient Damage Choking	0 0 0.20 0

N/A = Not Available

CHAPTER 3

THE EXPERIMENTAL SETUP AND PROCEDURE

3.1 The Experimental Facilities

The test equipments were located on pipe line at fluid test department on the factory floor of DoğuşVana A.Ş. The test setup is shown as in Figure 3.2. Also a picture of the test zone shown in Figure 3.1.

There are two different pumps in the test facilities; sump pumps are used for low flow rates and the centrifugal pumps are for high flow rates. The reason for that is to increase operational range of the facility with increased sensitivity for flow rate reading.

In the test facility, specification of the sump pumps are 50.08 kW, 110m^3/h and the specifications for the centrifugal pump are 250 kW, 2000m^3/h. These pumps were manufactured by "VANSAN" and "STANDART POMPA" respectively and controlled by a variable frequency drive.

Three different flow meters were used in the test setup. Note that as the valve opening decreases smaller flow meters are preferred due to higher accuracy. SIEMENS MAG 5100 DN500 flow meter (max 7063m^3/h) was used for the high flow rate as seen in Figure 3.3. KROHNE OPTIFLUX 2000 DN 300 (max 2000m^3/h) and DN 150 (max 400m^3/h) flow meters were used for the medium and low flow rates.

Figure 3.1 Test Zone

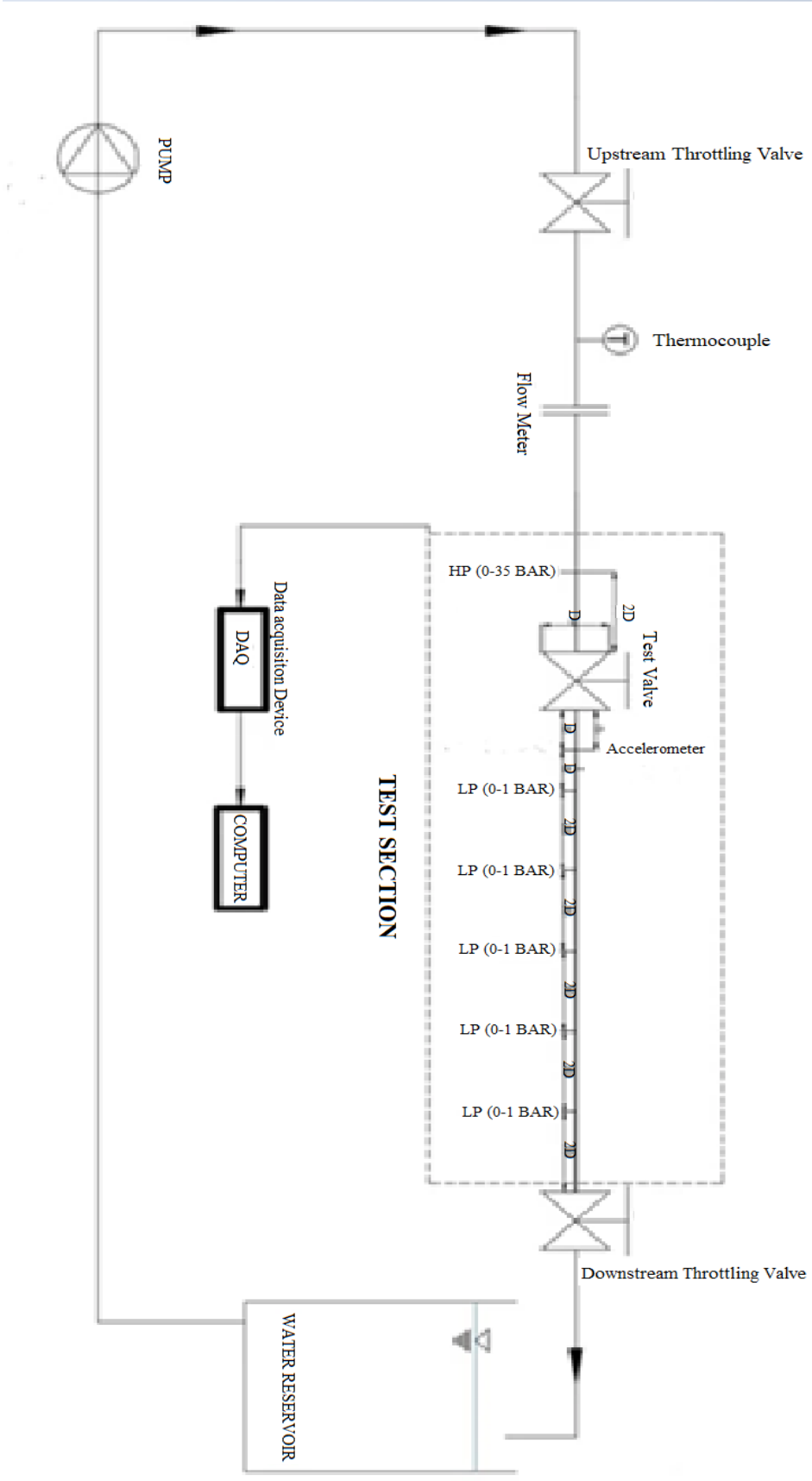

Figure 3.2 Experimental Set-up

Figure 3.3 Siemens MAG 5100 Flow Meter

DN500 PN16 butterfly valve and gate valve are used to lead to the test section from different pumps. Apart from these, a throttling valve is added downstream of the test setup to control the pressure differential associated with cavitation throughout the test section. This valve ensures to reach to desired cavitation level (incipient, constant, etc…)

Thermocouple made by ELİMKO company is used to measure water temperature which is needed to find the vapor pressure where cavitation highly which depends on.

Figure 3.4 Water Temperature Measurement by a Thermocouple

3.1.1 The Test Section

The upstream and downstream pressure tap locations shall conform with the test specimen (valve) diameter. According to standard (ISA), the upstream pressure tap and downstream pressure tap shall be located 2 nominal diametersupstream of the test specimen and 6 nominal diametersdownstream of the test specimen. It is important for test quality to leave a straight pipe length of at least 18 nominal diameters before the upstream pressure tap and 1 nominal diameter after the downstream pressure tap. In addition, 6 pressure taps are made to examine pressure changedownstream of the valve. One of them is located 1 nominal diameter away from the test valve, the others are placed 2 diameters away from the test specimen and each other. These pressure taps and accelerometerposition are summarized on Figure 3.5 and picture of sensor location on Figure 3.6

Pressure transducers used to measure the gauge pressure are OMEGA brand and type of PXM419-035BG10V and PXM419-001BG10V. Upstream and downstream pressure transducer have a range of 0-35 bar and 0-1 bar respectively.

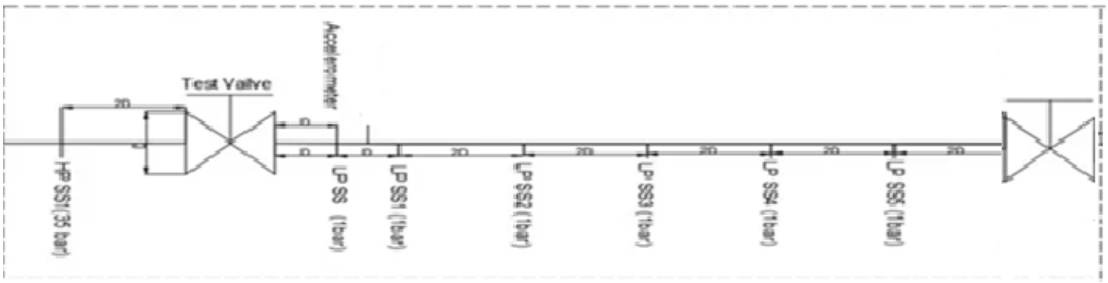

Figure 3.5 Position of the Sensors

Figure 3.6 Sensors on the Downstream Pipeline

An accelerometer that measures vibration is used for detecting cavitation intensity and limits. That is rigidly mounted on the pipe wall downstream of the test specimen. An ultrasonic gel between the accelerometer and the pipe wall is applied for better sensitivity. The location of the accelerometer is important, according to ISA standards the position of the accelerometer should be connected downstream about 1 diameter distance after the test specimen.

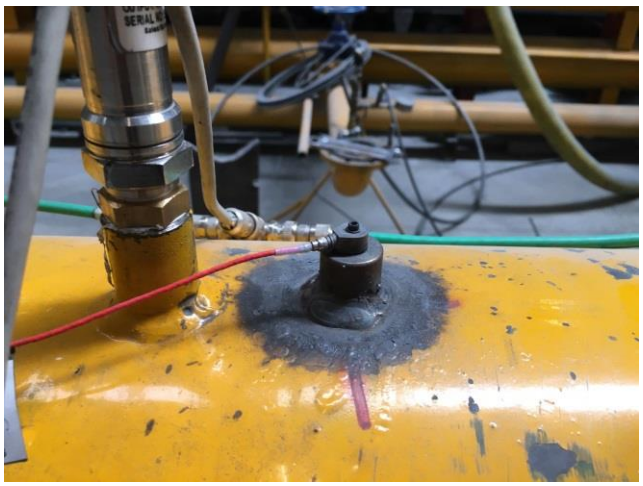

Figure 3.7 CavitationSensing Accelerometer (Endevco, type 7250B-10)

Combination of cavitation detection system as the shown in Figure (3.8).

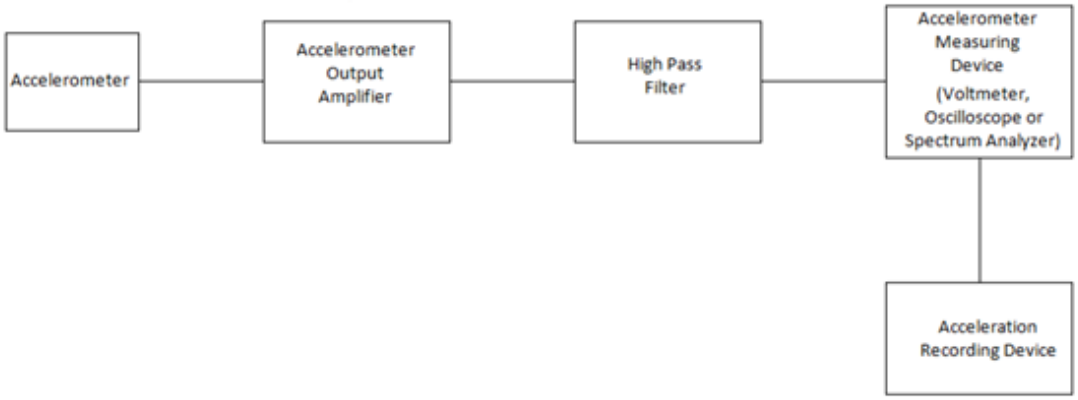

Figure 3.8 Cavitation Detection System (ISA)

The accelerometer error should be held between ±5%. to detect cavitation correctly. A high pass filter is used to remove low frequency (<5 kHz) vibrations to filter the background and turbulent flow noise.

3.2 Experimental Procedure

The cavitation in valves are measured according to certain test standard and procedures. The test steps for cavitation analysis and test procedure were explained in following paragraphs.

3.2.1 Procedure of Cavitation Analysis

- Valve coefficient (Cv) and Valve loss coefficient (K) are determined experimentally under specific flow conditions and opening ratio.
- The valve cavitation characteristic values (incipient, critical, etc.) are determined experimentally at specific flow conditions.
- Cavitation limits of the larger diameters and pressures are calculated by the size scale effect (SSE) and pressure scale effect (PSE).
- The desired application sigma value is compared with the experimental sigma values determined.
- If the desired sigma equal to or bigger than the experimental sigma value, the valve is in the safety cavitation region and is assumed to be working safely.

3.2.2 Test Procedure

- The valve should be tested at 20%, 30%, 40%, 50%, 60%, 70%, 80%, 90% and 100% opening rates. However, these opening ratios may vary according to the geometric structure of the valve. (Depending on geometric design, the plunger valve may not be opened 100%)
- Air in the pipeline must be removed by passing water at a high flow rate for at least 1 minute through the test setup.
- The downstream throttling valve should be fully open, or in the opening ratio that creates cavitation in the test valve.
- During a test, the upstream pressure sensor, downstream pressure sensor, flow meter, thermocouple, and accelerometer levels should be recorded with sample rates required for the aim of the test.
- To detect inflection points in the accelerometer &sigma curves, constant pressure must be maintain at the upstream reference section, the downstream throttle valve should be throttled down slowly, increasing the pressure difference from minimum to maximum.

3.3 Frequency Analysis for Cavitation Detecting

The explosions of vapor bubbles caused by cavitation occur at very high frequencies. Since this event happens very quickly, it is very difficult to detect it in a time series. For this reason, it is necessary to examine this signal in the frequency domain. Time series were transformed by Fourier transformation (FFT) so that frequency spectra were obtained.

The following Equation (3.1) defines the two-sided Fourier transform where f is frequency and t is time. As an example to this transformation is given in Figure (3.4) where a time domain top-hat function looks like a sombrero in the frequency domain;

$$X(f) = F(x(t)) = \int_{-\infty}^{\infty} X(t) e^{-j2\pi f t} dt \tag{3.1}$$

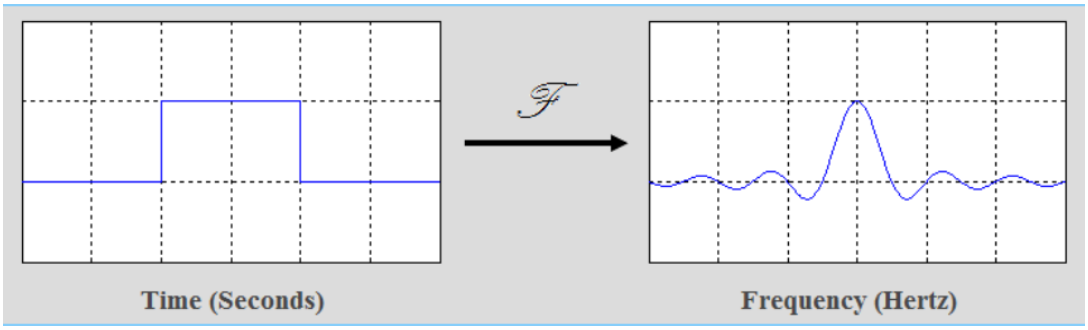

Figure 3.9: Transforming of Time to Frequency by FT

Frequency domain analysis may be giving us apparent frequency components, but does not tell us anything about the power of each component. Power of a vibration signal becomes obvious when Power Spectrum Density (PSD) is calculated. The power spectrum describes the energy distribution of a time series in the frequency domain and described as in Equation (3.2). The PSD measures the signal power per unit bandwidth for a time series in V^2/Hz. If the PSD is represented in a decibel (dB), the corresponding unit for the PSD is V/sqrt(Hz).

$$E = \int_{f_1}^{f_2} PSD(f)\, df \tag{3.2}$$

CHAPTER4

RESULT AND DISCUSSION

In this chapter, flow performance and cavitation detection of Plunger valve are experimentally studied and analyzed. The purpose of this analysis is to experimentally examine and discuss the responses of the valve at different opening ratio.

4.1 Pressure Drops Performance

The pressure-location relationship (a.k.a. pressure recovery) of the flow downstream of a plunger valve is shown with the hydraulic grade line in Figure 4.1. Each hydraulic grade line represents different opening ratios. As the opening ratio increases, the static pressure of the water gets closer the vapor pressure (22,7 mbar) and brings the risk of cavitation. Downstream of the plunger valve exit, the first 1D is the most risky location for cavitation, where the velocity is maximum and the pressure is minimum. After the 4D, pressure recovery is almost complete and hydraulic grade lines gets a constant value.

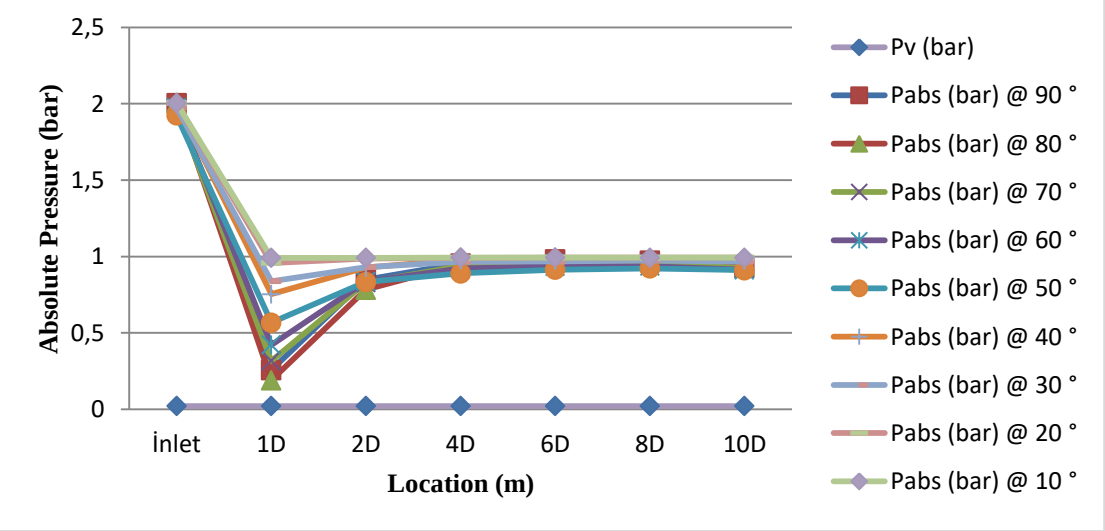

Figure 4.1 : Pressure Distribution at Different Opening Ratio for DN 250 Plunger Valve

4.1.1 Effect of Reynolds Number on Loss Coefficient

Reynolds numbers & Loss coefficient relationships were investigated on two different diameters and different opening ratios in Figures 4.2 and 4.3. The loss coefficients don't change significantly when the Reynolds Number is increased. The loss coefficient remained practically constant at Reynolds numbers greater than 400000 in Figure 4.2 and greater than 500000 in Figure 4.3 The reason for this is that the boundary layers are not thick enough to create any effect on the flow, therefore there is no change in the pressure difference (Carretero and Breuer, 2000).

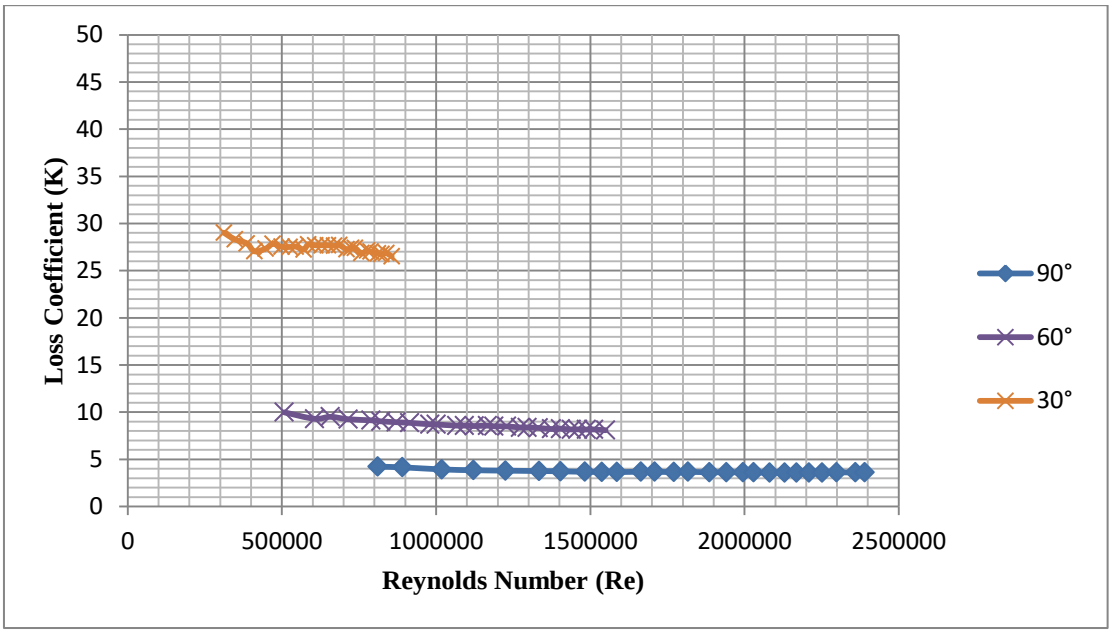

Figure 4.2: Variations of Loss Coefficient with Reynolds Number for DN 300 Plunger Valve (No Lattice)

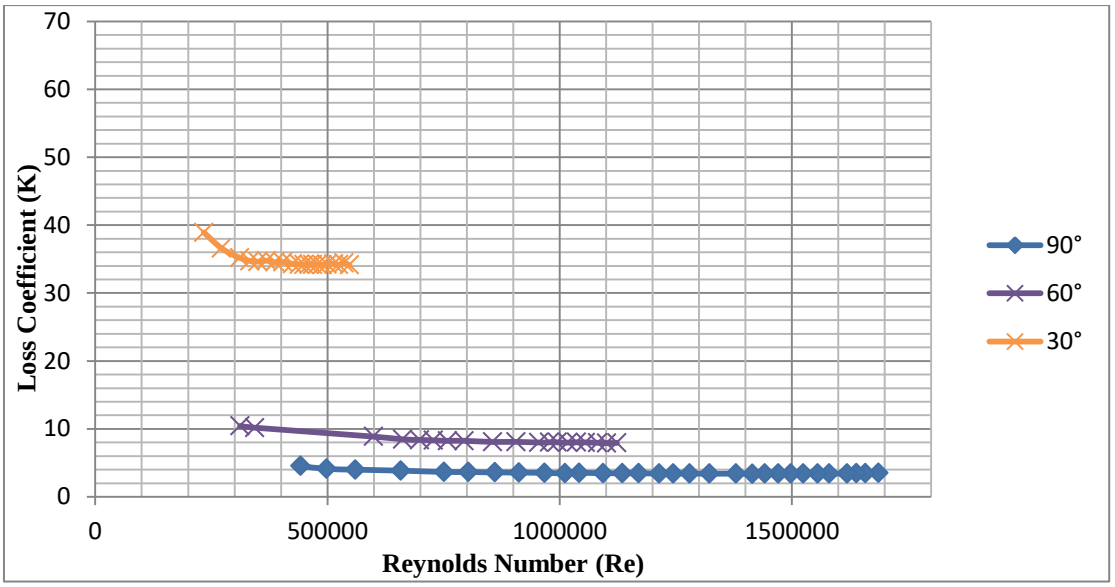

Figure 4.3: Variations of Loss Coefficient with Reynolds Number for DN 200 Plunger Valve (No Lattice)

4.1.2 Effect of Valve Opening Ratio on Loss and Flow Coefficients

The loss coefficient, which is a dimensionless coefficient, is a very important parameter to compare the performance of valves. This parameter describes the flow resistance of the valve for different opening ratios. Figure 4.4 is revealed the pressure drop performance of the DN250 plunger valve with and without a cavitation lattice. In order to clarify the relationship of loss coefficients with the opening ratio, it is shown in the semi-logarithmic measurement. It is seen that the lattices has greater effect on pressure loss at higher openings (higher flow rate). The reason for this is the resistance of cavitation lattice against flow. As can be seen in the graph, there is no significant difference between DV 20 and DV40 cavitation lattice, but it has been observed that the orifice type lattices have a higher loss coefficient after 50 % opening ratio.

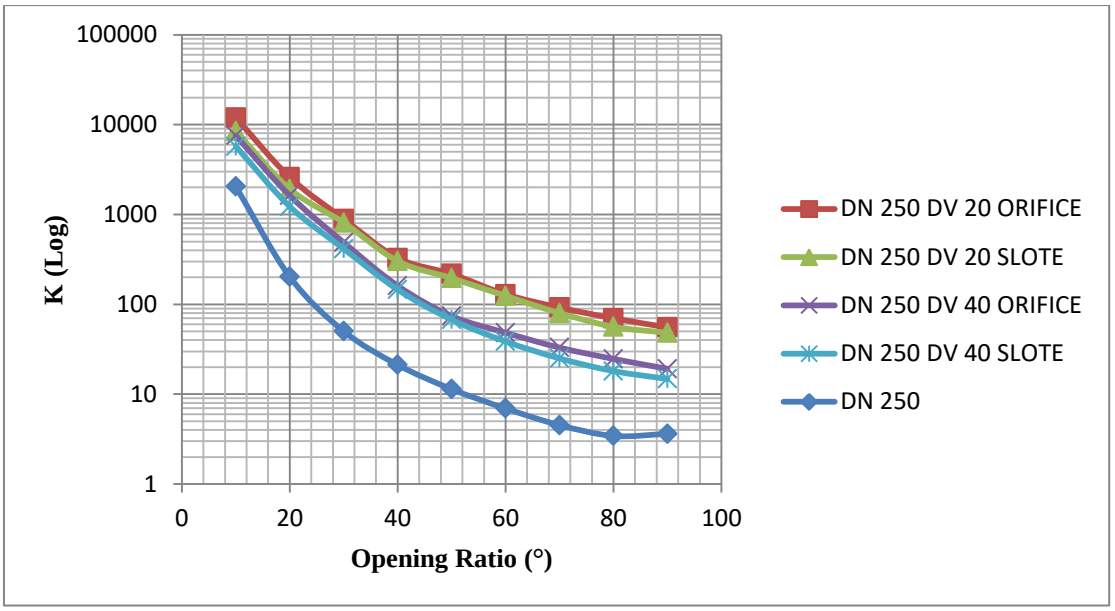

Figure 4.4: Distribution of Loss Coefficient with opening ratio for DN 250 Plunger Valve and Different Cavitation Lattice

Flow coefficient does not contain any information other than loss coefficient. However, the flow coefficient can be useful in engineering applications. For this reason, information about flow coefficients is shown in the appendix section.

4.2 Cavitation Detection

4.2.1 Investigating of Cavitation with Frequency Analysis

The frequency response of the plunger valve under initial and critical cavitation is examined at different opening ratios in Figure 4.5 and Figure 4.6. As the opening ratio decreases, the cavitation intensity tends to decrease. This is an expected outcome, since pressure bottom occurring at vena contracta is not very low for low flow rates. In Figure 4.6, resonances were observed in the frequency ranges of 5 kHz and 12 kHz at 90%, 70% and 50% openingratio.

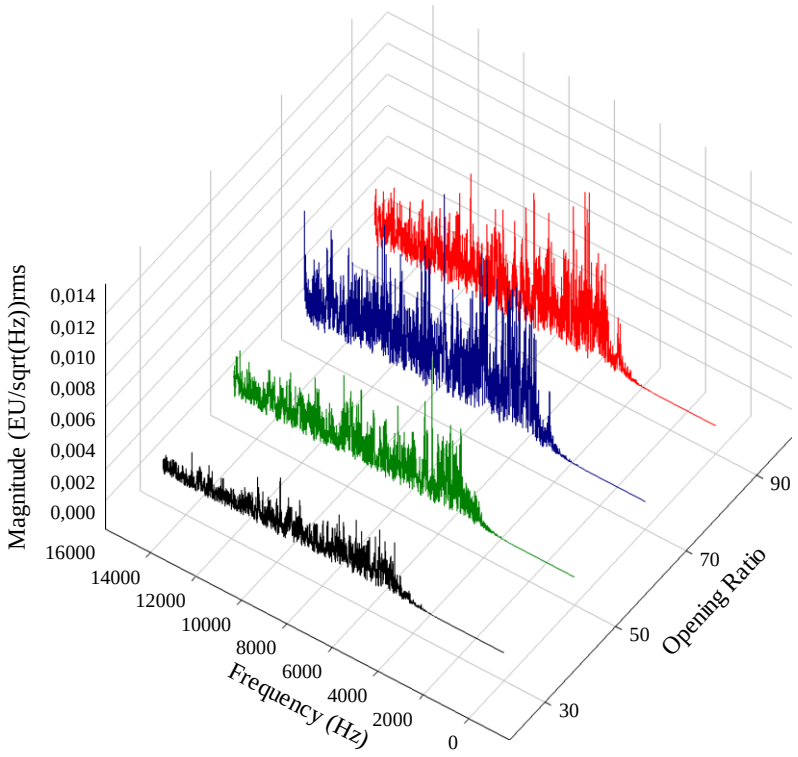

Figure 4.5: Accelerometer Frequency Response under Incipient Cavitation for DN 250 Plunger Valve with Different Opening Ratios

In Figure 4.6, frequency analysis of critical cavitation is examined. Critical cavitation has been found to contain more intense cavitation noise. However, Critical cavitation occurred in lower frequency ranges (5 Khz to 8 kHz). This is because larger bubbles create lower vibration frequencies. That is, bubble diameters in the incipient cavitation are lower than in critical cavitation (Ulanicki, Picinali, and Janus, 2015).

In Figure 4.7 and Figure 4.8, frequency analysis of four different cavitation lattices at 70% opening ratio under incipient and critical cavitation were examined. It isfound that cavitation intensity is higher in DV 40 lattice than DV 20 lattice. This occurs due to the pressure difference. DV 40 lattice has a hole and slot area more than DV20 therefore cavitation intensity is higher.

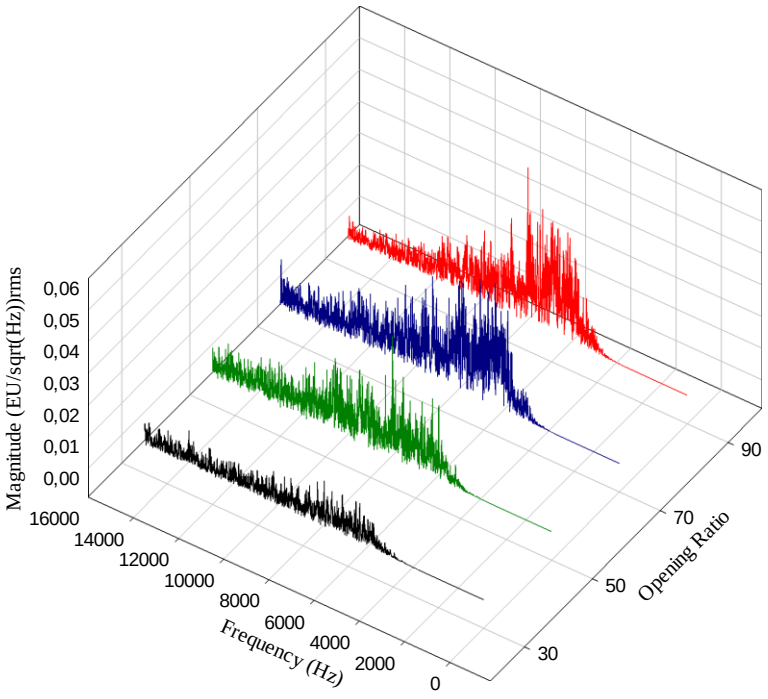

Figure 4.6: Accelerometer Frequency Response under Critical Cavitation for DN 250 Plunger Valve with Different Opening Ratios

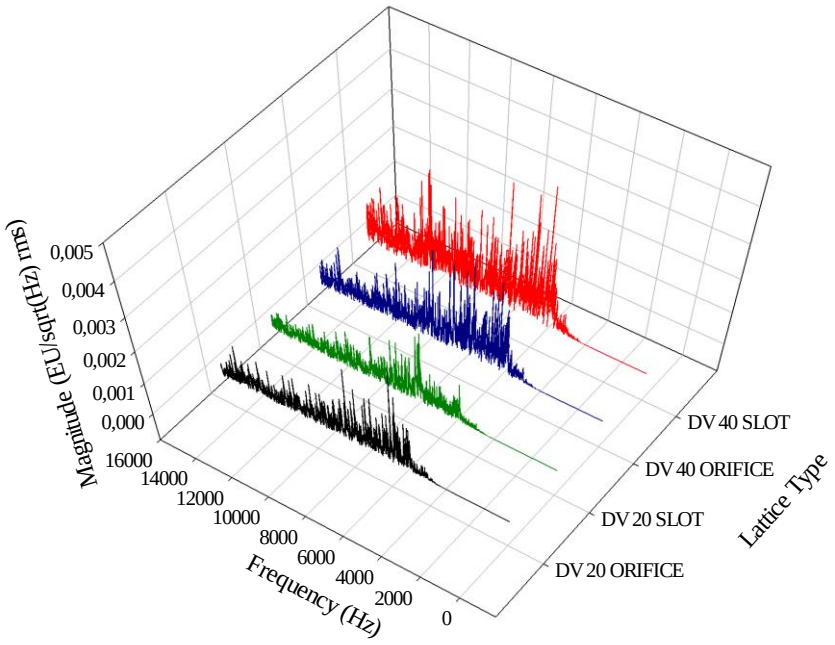

Figure 4.7: Accelerometer Frequency Response under Incipient Cavitation for DN 250 Plunger Valve at %70 opening ratio with Various Lattice Types

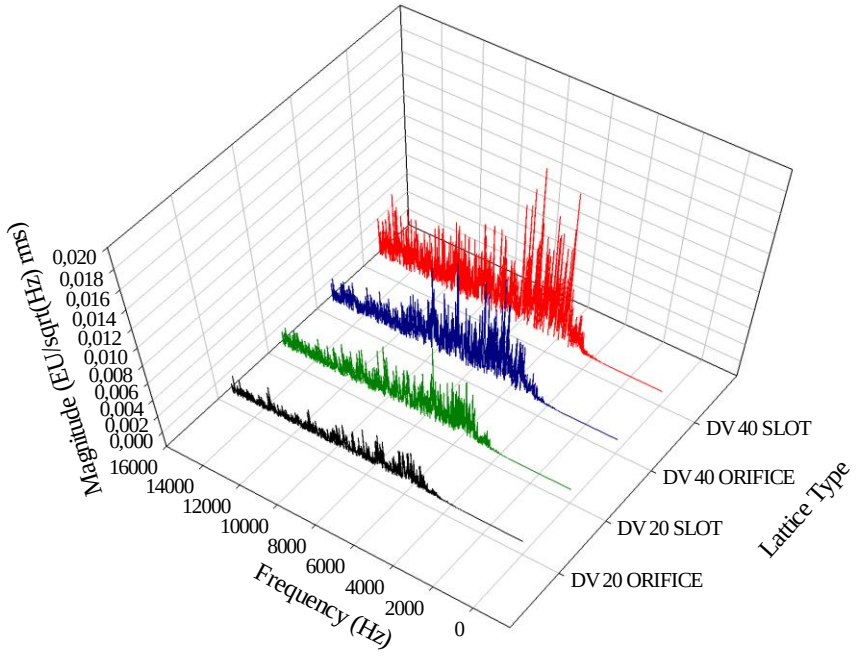

Figure 4.8: Accelerometer Frequency Response under Critical Cavitation for DN 250 Plunger Valve at %70 opening ratio with Various Lattice Types

Power spectrum diagrams for the same readings are presented in Figure 4.9, 4.10, 4.11 and 4.12. Spectral energy was compared under incipient and critical cavitation at 90% and 30% opening rates in Figures 4.13 and 4.14. At 90% opening ratio, critical cavitation intensity reached -30 dB in the frequency range 6 - 7 kHz and it shows a drop for higher frequencies. That is an indication of energy containing larger bubble collapse. On the other hand, for incipient cavitation the vibration intensity can only reached -40 dB in the range 10-12 kHz, so it is much lower than the critical cavitation and shows no drop for higher frequencies. This indicates that energy content of the bubbles are not only lower but also large and small bubbles have almost the same amount of power. As for the %30 opening ratio shown in Figure 4.10, critical cavitation intensity reached -40 dB in the frequency range 6 - 7 kHz and shows no drop for higher frequencies. This indicates that same behavior in incipient cavitation at 90% opening ratio. For incipient cavitation the vibration intensity can only reached -60 dB in the range 6 – 7 kHz and it shows a drop for higher frequencies. This indicates that same behavior in critical cavitation at 90% opening ratio.

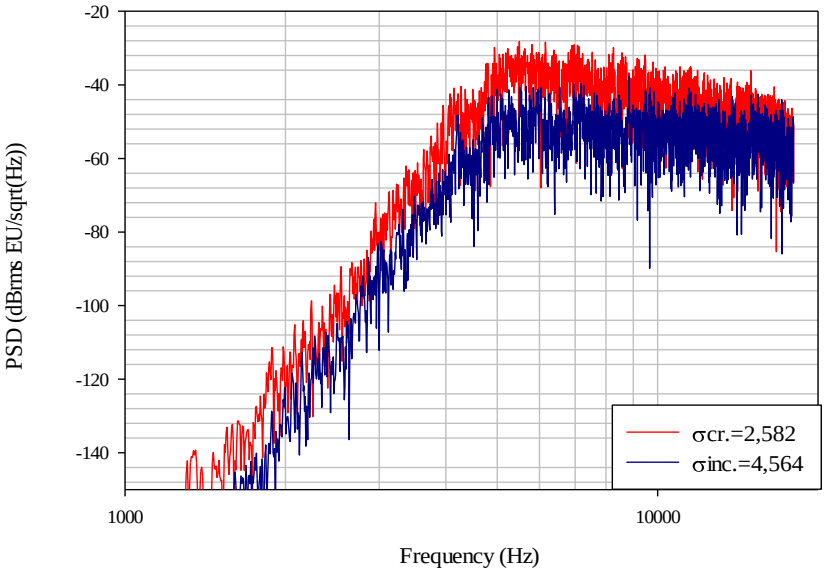

Figure 4.9: Comparison the Cavitation Levels on Power Spectrum for DN 250 Plunger Valve (No Lattice) at 90% Opening Ratio

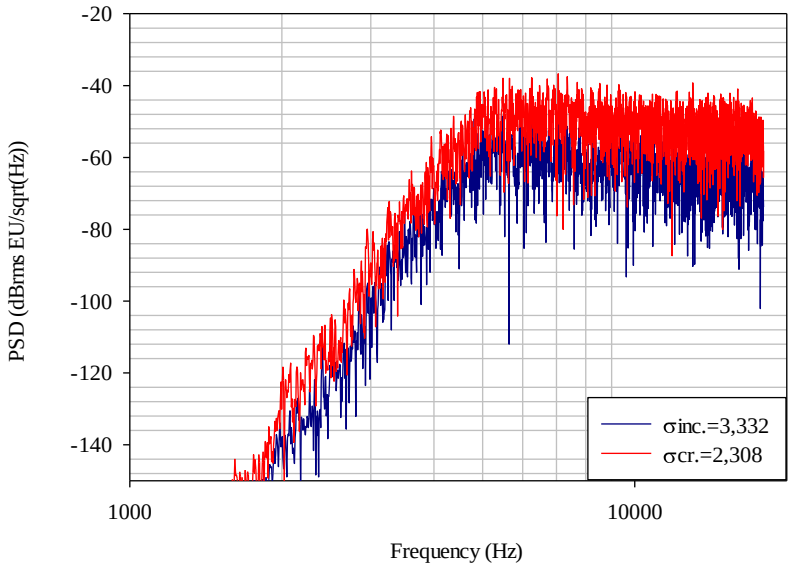

Figure 4.10: Comparison the Cavitation Levels on Power Spectrum for DN 250 Plunger Valve (No Lattice) at 30% Opening Ratio

Spectral energy of cavitation under the same valve openings for various lattices were examined in Figures 4.11 and 4.12. In Figure 4.11 examined under the incipient cavitation, it is seen that the energy levels affected by each lattice are close to each other. However, the spectral energy of cavitation is higher in slot type cavitation lattice, while it is lower in orifice type cavitation lattice. In Figure 4.12 examined under critical

cavitation, the effect of lattice types on cavitation is visually clearer.

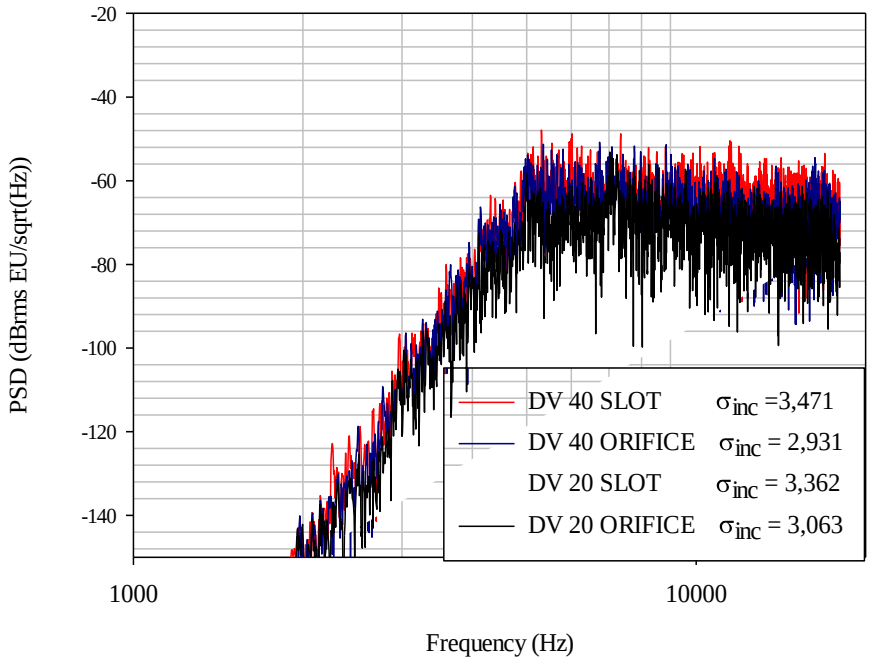

Figure 4.11: Power Spectrum distribution for DN 250 Plunger Valve with Various Lattice Type under Incipient Cavitation at 90 % Opening Ratio

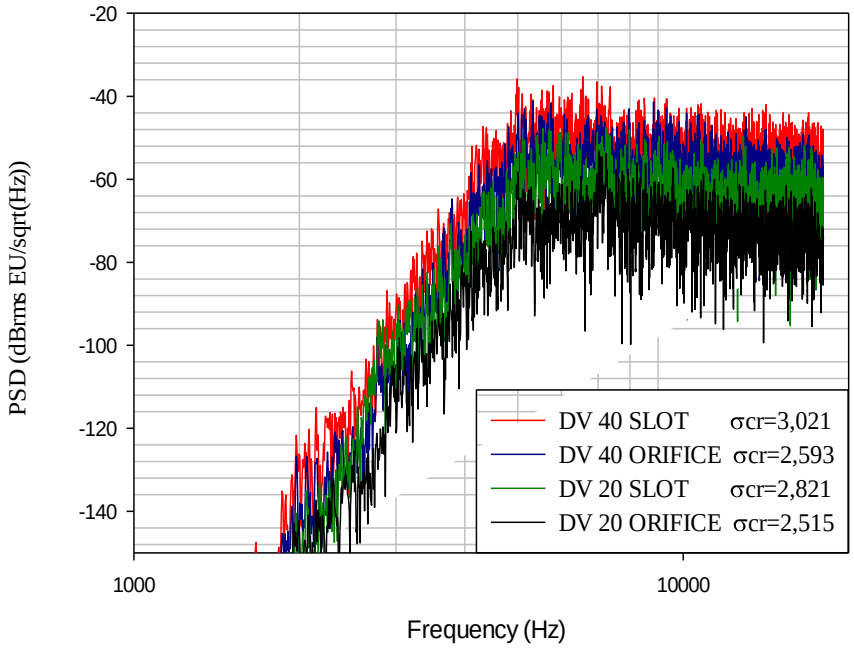

Figure 4.12: Power Spectrum distribution for DN 250 Plunger Valve with Various Lattice Type under Critical Cavitation at 90 % Opening Ratio

4.2.2 Detecting Cavitation Limits

Figure 4.13, 4.14.4.15 and 4.16 show the incipient and critical cavitation indexes of a plunger valve without a lattice. Cavitation indexes on the X-axis are compared against the noise of vibrations on the Y-axis. Blue marks represent the non-cavitation line, red marks the incipient cavitation, and green marks the critical cavitation. Sharp transitions were observed between the cavitation limits. The marks are combined with a linear line and their intersection determines the cavitation limits. Table 4.1 shows the cavitation index and noise levels between 90% and 20% opening ratio. Cavitation limit indexes and graphics of cavitation lattices are in the appendix section.

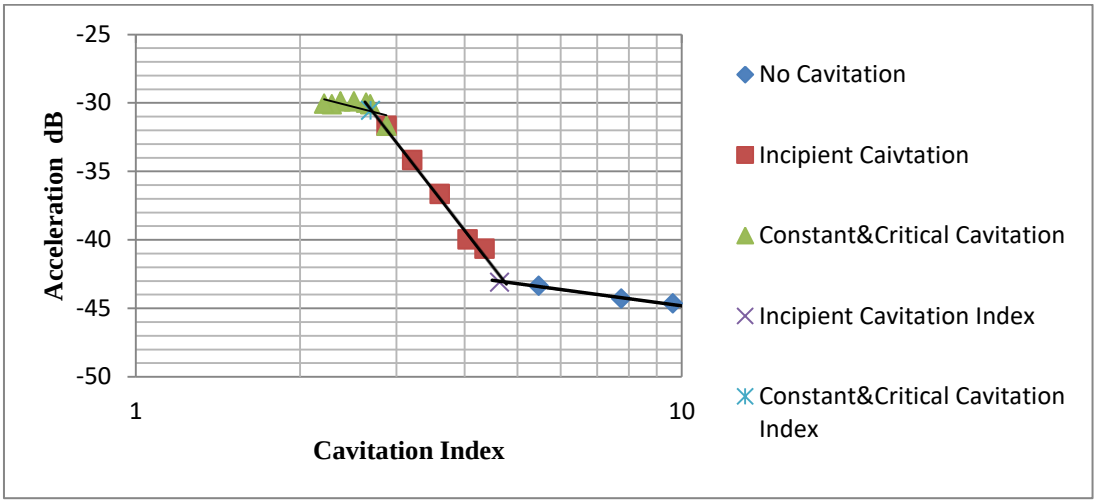

Figure 4.13: Detecting Incipient and Critical Cavitation at 90° opening ratio for DN250 Plunger Valve (No Lattice)

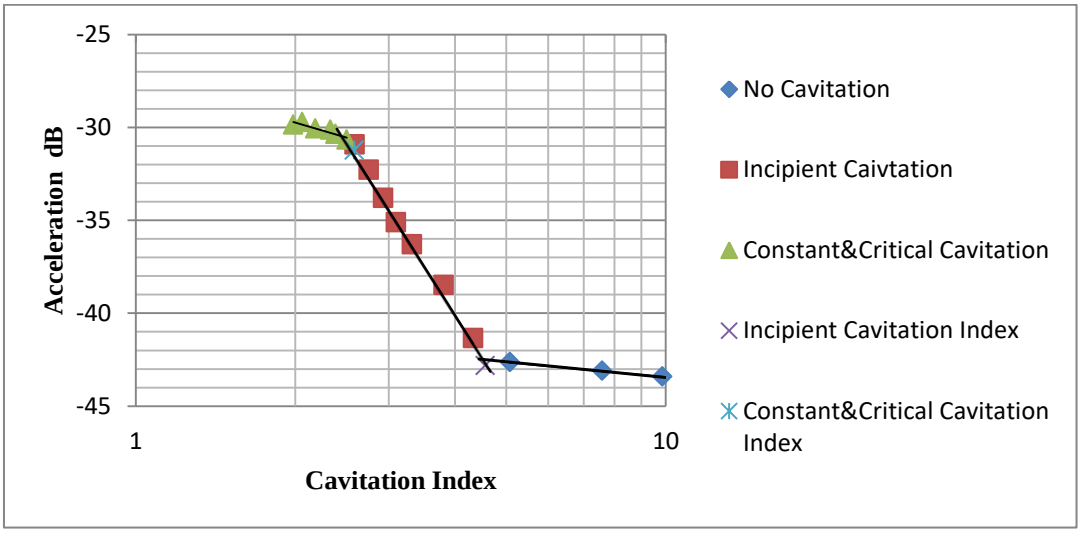

Figure 4.14: Detecting Incipient and Critical Cavitation at 70° opening ratio for DN250 Plunger Valve (No Lattice)

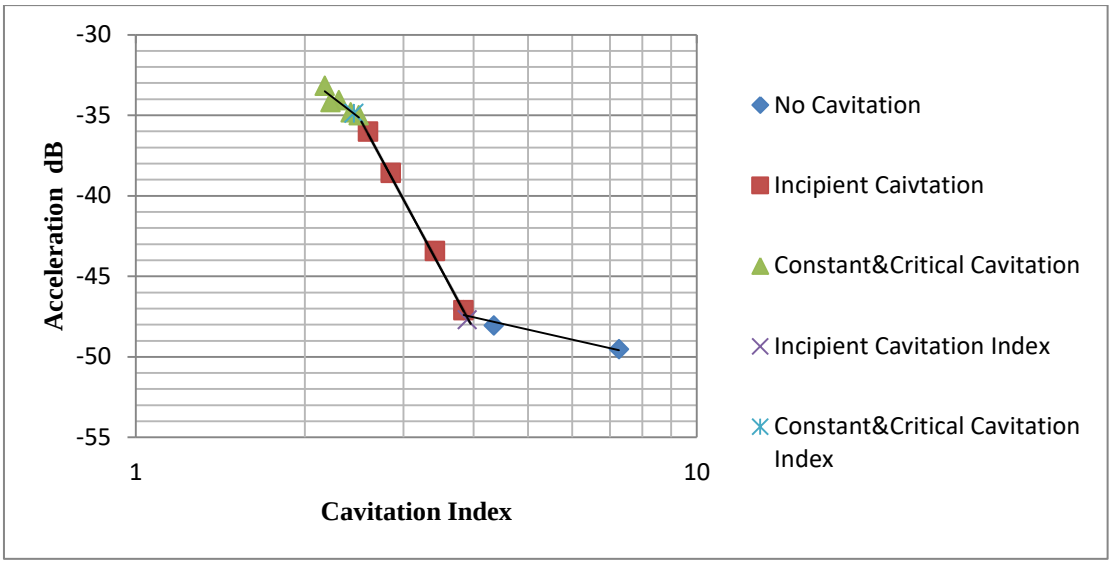

Figure 4.15: Detecting Incipient and Critical Cavitation at 50° opening ratio for DN250 Plunger Valve (No Lattice)

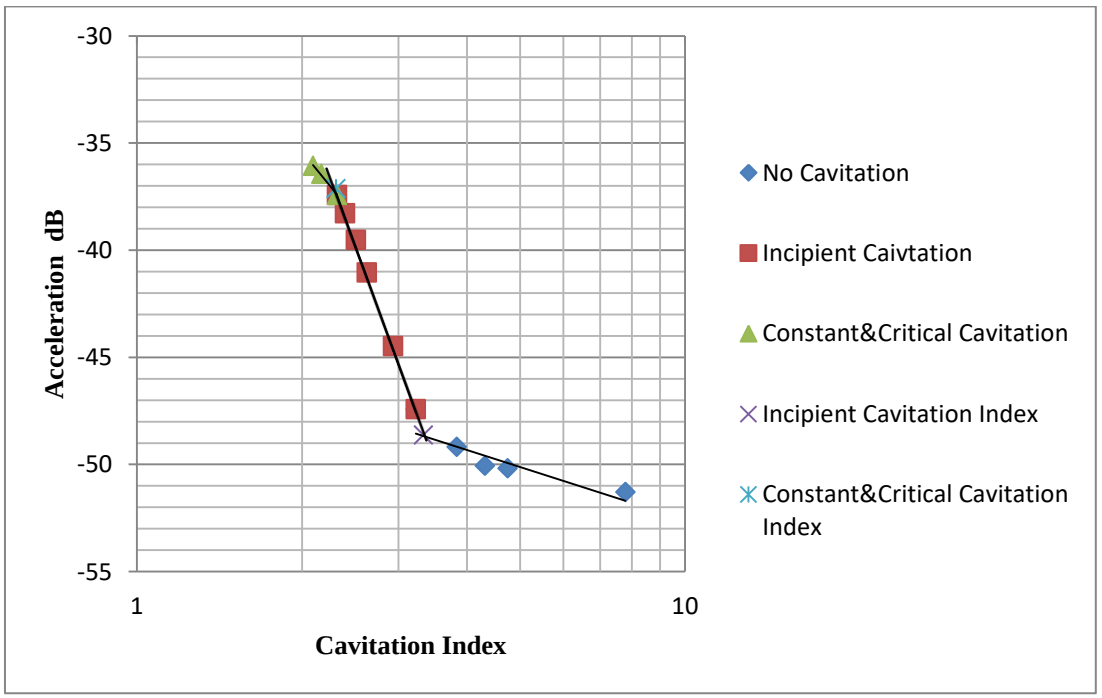

Figure 4.16: Detecting Incipient and Critical Cavitation at 30° opening ratio for DN250 Plunger Valve (No Lattice)

TABLE 4.1 :Value of Cavitation Levels and Acceleration dB for DN 250 Plunger Valve (No Lattice)

Openings [°]	IncipientCavitation Index	Acceleration dB	Critical Cavitation Index	Acceleration dB
90	4,63	-43,11	2,69	-30,55
80	4,61	-41,60	2,64	-30,64
70	4,56	-42,83	2,52	-31,22
60	4,40	-46,20	2,49	-32,40
50	3,90	-47,71	2,44	-34,88
40	3,44	-52,93	2,35	-38,319
30	3,33	-48,62	2,30	-40,12
20	2,97	-63,54	2,26	-45,42

In Figure 4.17, the initial and critical cavitation limit indexes of a plunger valve without a lattice are shown according to the opening ratios.The area above the incipient cavitation curve and up to the critical cavitation curve is the safe operating range. The region below the critical cavitation curve is the risky operating range. It was observed that after 60% opening, the distance between the two curves started to decrease. As the opening ratio decreases, the safe operation range increases.

4.2.3 Characteristic of Incipient and Critical Cavitation

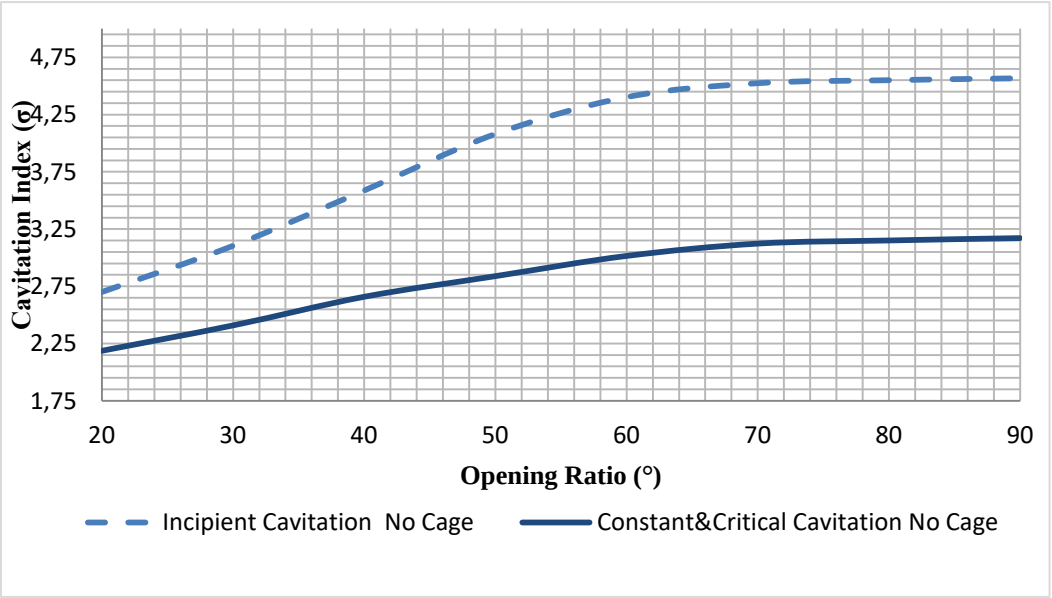

Figure 4.17: Cavitation Limits for DN 250 Plunger Valve (No Lattice)

In Figure 4.18, the cavitation limits of DV 20 orifice and slot lattice at different opening ratios are examined. When orifice and slot type lattice are compared, it was seen that orifice type lattice contains smaller cavitation indexes. This means that this orifice type produces a better solution as it creates a larger safe cavitation range than the slot type. In Figure 4.19, DV 40 orifice and slot lattices are compared. Since the number of holes and slots is higher than DV 20, it creates a high pressure difference. Thus, cavitation risk is greater than DV 20. In Figure 4.20 and Figure 4.21, the same types of lattice are compared according to the number of orifice and slots. Since the flow-through area of the slot type lattices is larger than the orifice lattices, the pressure difference is high. This indicates that the risk of cavitation is also high.

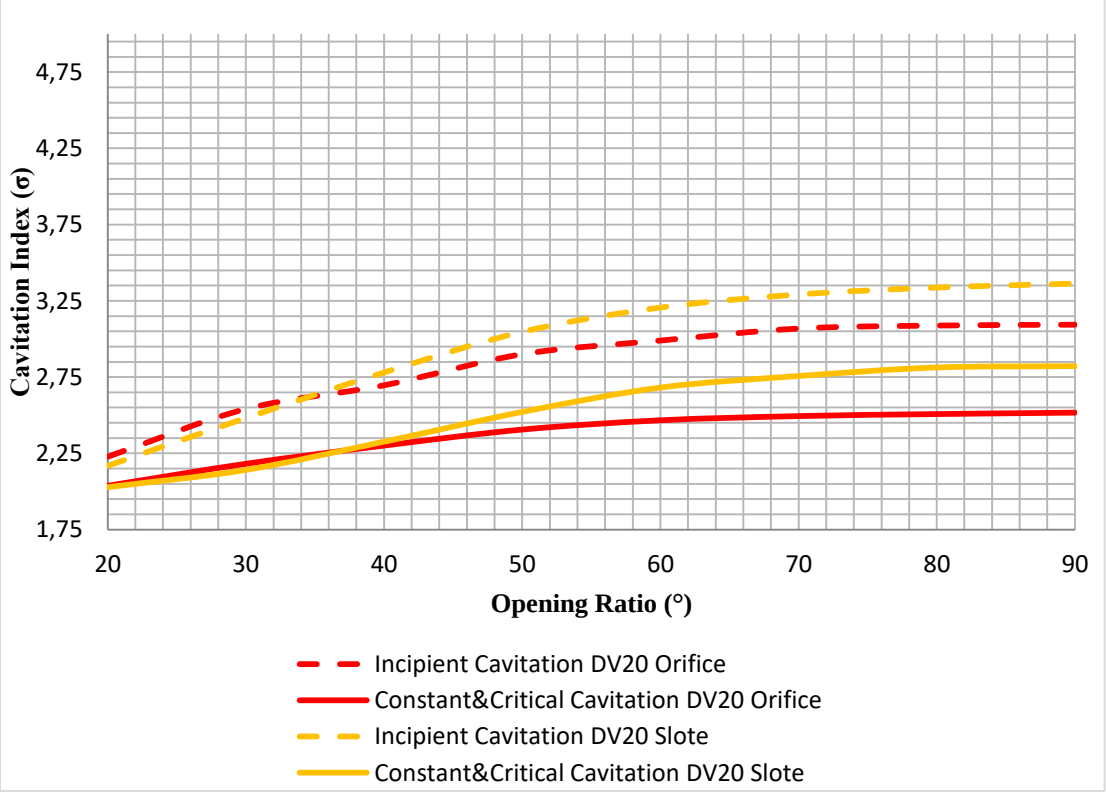

Figure 4.18: Cavitation Limits for DN 250 Plunger Valve with DV20 Orifice & Slot

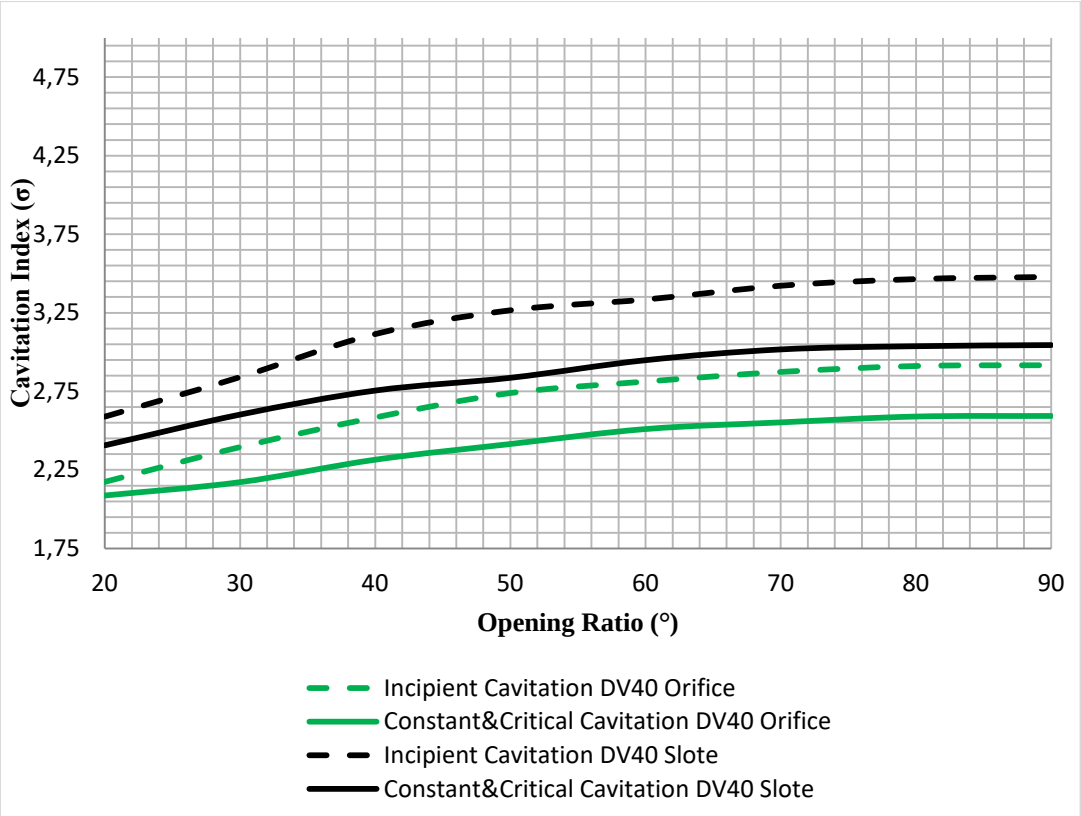

Figure 4.19: Cavitation Limits for DN 250 Plunger Valve with DV40 Orifice & Slot

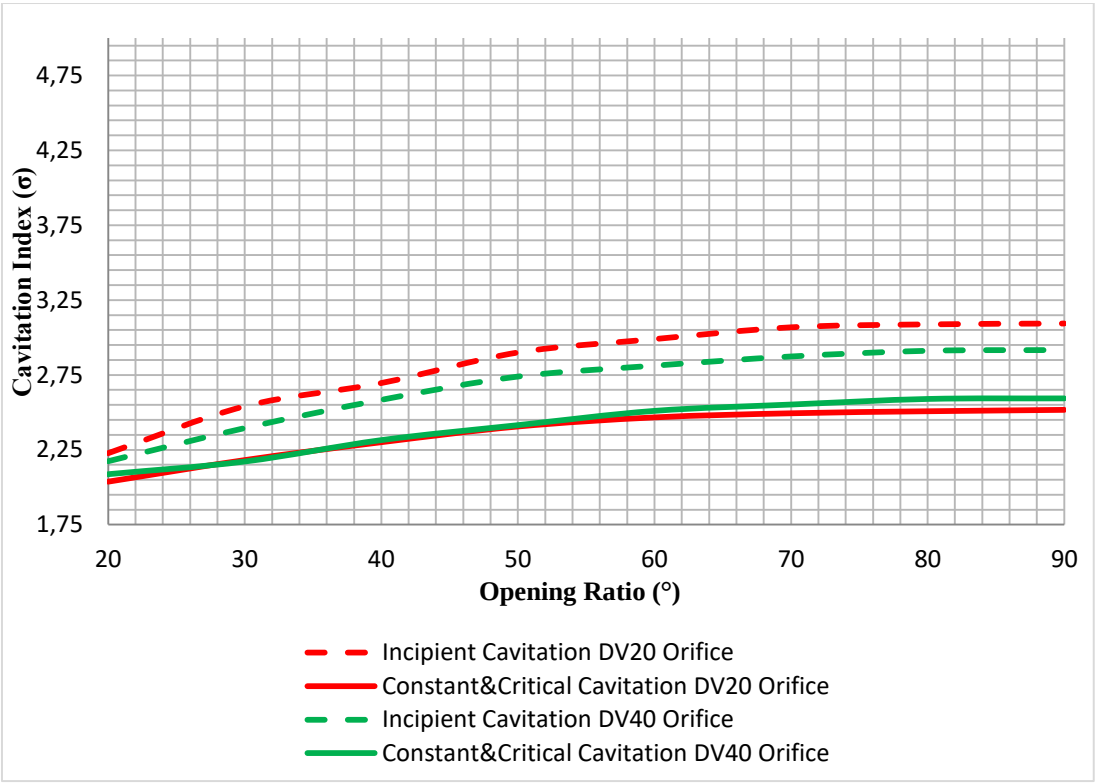

Figure 4.20: Cavitation Limits for DN 250 Plunger Valve with DV40&DV20 Orifice

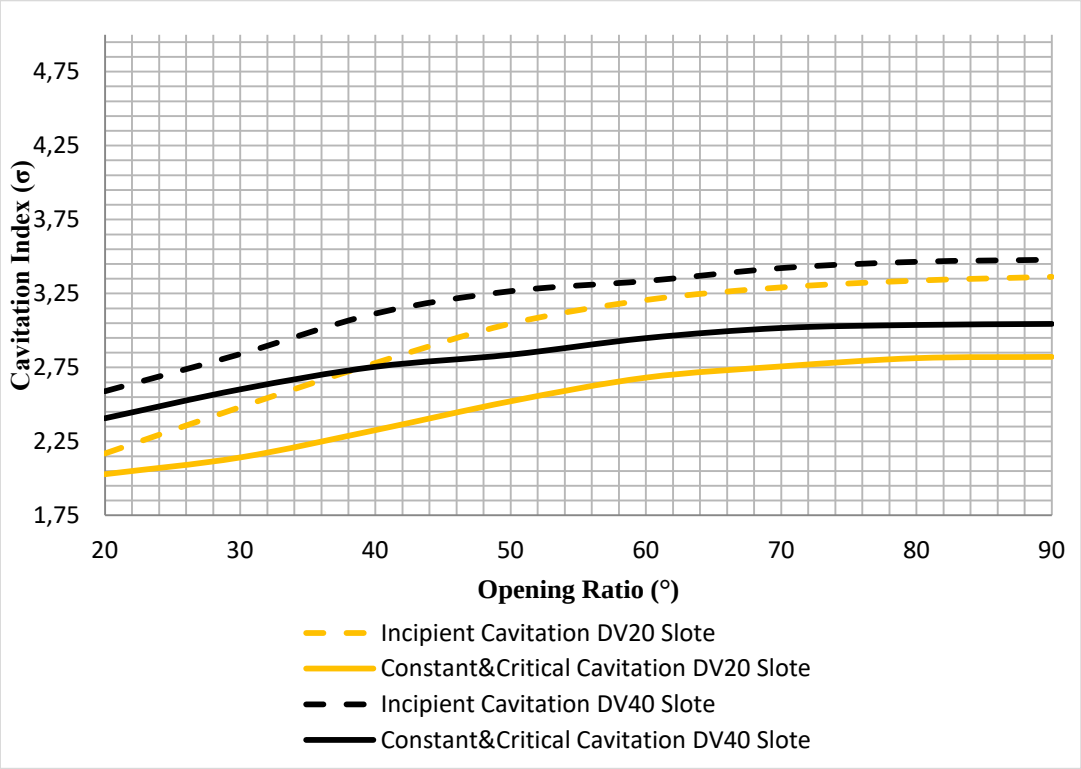

Figure 4.21: Cavitation Limits for DN 250 Plunger Valve with DV40&DV20 Slot

4.2.4 Size and Pressure Scaling Effect

In this section, cavitation limits of valves under different diameter and pressure conditions are determined with the effects of size and pressure.

In Table 4.2 and Table 4.4, cavitation indexes of DN 250 plunger valve are converted to DN 200 and DN 300 plunger valve with size scale effect. Reference cavitation indices (σ_{iref} and σ_{cref}) represent experimental cavitation indices. DN200 and DN 300 parameters are obtained by calculating according to equations between (2.8) and (2.12). In addition, in order to check the accuracy of this calculation, the experimental values of DN200 and DN300 values are sized and compared and the error ratios are shown in Table 4.3 and Table 4.5.

Table 4.2 : Cavitation limits of DN200 Plunger Valve with Size Scale Effect.

			DN 250 (Experimental)		DN 200 (SSE)		DN 200 (Experimental)	
Openings [°]	**Y**	**SSE**	σ_{iref}	σ_{cref}	σ_{iSSE}	σ_{cSSE}	σ_{iref}	σ_{cref}
90	0,22	0,95	4,56	3,17	4,49	3,62	4,53	3,65
80	0,21	0,93	4,55	3,15	4,48	3,59	4,50	3,62
70	0,20	0,95	4,52	3,12	4,42	3,57	4,44	3,60
60	0,18	0,96	4,40	3,01	4,26	3,38	4,27	3,42
50	0,16	0,96	4,08	2,83	3,97	3,10	3,98	3,14
40	0,14	0,96	3,58	2,65	3,50	2,75	3,50	2,78
30	0,11	0,97	3,10	2,40	3,05	2,46	3,05	2,50
20	0,08	0,92	2,70	2,18	2,53	2,14	2,55	2,12

Table 4.3 : Error rate of comparing SSE and Experimental (DN 200)

	ERROR %	
Openings [°]	σ_{iref}	σ_{cref}
90	-0,86	-0,70
80	-0,55	-0,66
70	-0,45	-0,68
60	-0,25	-1,07
50	-0,26	-1,23
40	0,12	-0,95
30	-0,14	-1,77
20	-0,80	0,91

Table 4.4 : Cavitation limits of DN 300 Plunger Valve with Size Scale Effect

			DN 250 (Experimental)		DN 300 (SSE)		DN 300 (Experimental)	
Openings [°]	**Y**	**SSE**	σ_{iref}	σ_{cref}	σ_{iSSE}	σ_{cSSE}	σ_{iref}	σ_{cref}
90	0,22	1,04	4,56	3,17	4,71	3,26	4,83	3,32
80	0,21	1,04	4,55	3,15	4,69	3,23	4,76	3,27
70	0,20	1,04	4,52	3,12	4,65	3,20	4,74	3,23
60	0,18	1,03	4,40	3,01	4,51	3,08	4,57	3,11
50	0,16	1,03	4,08	2,83	4,17	2,89	4,23	2,92
40	0,14	1,03	3,58	2,65	3,65	2,70	3,67	2,71
30	0,11	1,02	3,10	2,40	3,14	2,43	3,18	2,47
20	0,08	1,01	2,70	2,18	2,72	2,20	2,75	2,20

Table 4.5 : Error rate of comparing SSE and Experimental (DN 300)

	ERROR %	
Openings [°]	**σ_{iref}**	**σ_{cref}**
90	-2,60	-1,90
80	-1,50	-1,17
70	-1,83	-1,05
60	-1,29	-1,12
50	-1,47	-1,18
40	-0,47	-0,39
30	-1,10	-1,31
20	-1,15	-0,18

In Table 4.6, the upstream pressure of the DN250 plunger valve was increased from 2 bar to 5 bar. With the pressure scale effect, new cavitation values were examined. Since the test setup could not provide an inlet pressure of 5 bar, comparison could not be made with experimental data. In Figure 4.25, cavitation indexes with inlet pressures of 2 and 5 bar and opening ratios are shown in the graph. The cavitation values increased with the increase in inlet pressure.

Table4.6 : Cavitation Limits at 5 bar Upstream Pressure with PSE

Openings [°]	**X**	**PSE**	**σ_{iref}**	**σ_{cref}**	**P1 (abs)**	**P1 (abs)**	**Pv @25°C**	**σ_i**	**σ_c**
90	0,14	1,138	4,56	3,17	2	5	0,024	5,06	3,47
80	0,14	1,138	4,55	3,15	2	5	0,024	5,04	3,44
70	0,14	1,138	4,52	3,12	2	5	0,024	5,01	3,41
60	0,14	1,138	4,40	3,01	2	5	0,024	4,87	3,29
50	0,14	1,138	4,08	2,83	2	5	0,024	4,50	3,09
40	0,14	1,138	3,58	2,65	2	5	0,024	3,94	2,88
30	0,14	1,138	3,10	2,40	2	5	0,024	3,39	2,60
20	0,14	1,138	2,70	2,18	2	5	0,024	2,93	2,35

CHAPTER5

CONCLUSION

The objective of this thesis is to detect the pressure drop performance and cavitation characteristics of a plunger valve as experimentally. Cavitation detections were carried out on DN 300, DN250 and DN200 plunger valves. The effects of different lattice types on pressure drops (loss coefficient) and cavitation were compared. The DN 250 plunger valve has been tested under 20% to 90% opening ratios with four different cavitation lattice (DV 20 orifice DV 20 slot DV 40 orifice DV 40 slot). The pressure drop performance has been characterized, as the number of slots and orificehole number increases, the pressure loss coefficient decreases,enabling the plunger valve to be used in applications with a wider control range. The loss coefficients at different opening ratios were examined with the Reynolds number. The loss coefficient is seen to be independent from Reynolds numbers after 800000 and 400000 for DN300 and DN200 plunger valves.

The second part of the thesis is the cavitation detection of the plunger valve. The vibration noise level was examined at high frequencies (5 - 18 kHz) with the accelerometer. Accordingly, the incipient cavitation and critical cavitation were determined and cavitation limits were established. In two lattice types, DV 20 slot and DV 20 orifice lattices are found suitable for the plunger valve to operate within wider cavitation limits. However, the DV 20 orifice provided better performance in terms of decreasing cavitation intensity, and also it has more safe operational range than the DV 20 slot.

The DN 250 plunger valve was taken as reference to the estimating the cavitation limits of DN 200 and DN 300 valves with the size scale effect.Error rates were obtained between estimated values and real values.These estimates show that by testing only one valve and reference the results of this valve, cavitation detection of larger (up to 914 mm) or smaller diameter valves can be made.

REFERENCES

Libera, G. 2015. “State of the Art and Perspectives on the Study of Valves Cavitation.” https://www.politesi.polimi.it/bitstream/10589/108793/1/2015_07_Libera.pdf.

Soyama, H., and J. Hoshino. 2016. “Enhancing the Aggressive Intensity of Hydrodynamic Cavitation through a Venturi Tube by Increasing the Pressure in the Region Where the Bubbles Collapse.” *AIP Advances* 6 (4). https://doi.org/10.1063/1.4947572.

J. Paul, Tullis. 1993. *Cavitation Guide for Control Valves*. *U.S Nuclear Regulatory Commission*. https://www.osti.gov/biblio/10155405.

Zhao, Rui, Rong qing Xu, Zhong hua Shen, Jian Lu, and Xiao wu Ni. 2007. “Experimental Investigation of the Collapse of Laser-Generated Cavitation Bubbles near a Solid Boundary.” *Optics and Laser Technology* 39 (5): 968–72. https://doi.org/10.1016/j.optlastec.2006.06.005.

Brennen, Christopher Earls. 2013. *Cavitation and Bubble Dynamics*. *Cavitation and Bubble Dynamics*. Cambridge University Press. https://doi.org/10.1017/CBO9781107338760.

Jablonská, Jana, Miroslav Mahdal, and Milada Kozubková. 2017. “Spectral Analysis of Pressure, Noise and Vibration Velocity Measurement in Cavitation.” *Measurement Science Review* 17 (6): 250–56. https://doi.org/10.1515/msr-2017-0030.

Meng, Jiang, Zhipeng Liu, Kun An, and Meini Yuan. 2017. “Simulation and Optimization of Throttle Flowmeter with Inner-Outer Tube Element.” *Measurement Science Review* 17 (2): 68–75. https://doi.org/10.1515/msr-2017-0009.

Samuel Martin, C., H. Medlarz, D. C. Wiggert, and C. Brennen. 1981. “Cavitation Inception in Spool Valves.” *Journal of Fluids Engineering, Transactions of the ASME* 103 (4): 564–75. https://doi.org/10.1115/1.3241768.

Ulanicki, Bogumil, Lorenzo Picinali, and Tomasz Janus. 2015. “Measurements and Analysis of Cavitation in a Pressure Reducing Valve during Operation a Case Study.” *Procedia Engineering* 119 (1): 270–79. https://doi.org/10.1016/j.proeng.2015.08.886.

Holl, J. W. 1960. “An Effect of Air Content on the Occurrence of Cavitation.” *Journal of Fluids Engineering, Transactions of the ASME* 82 (4): 941–44. https://doi.org/10.1115/1.3662809.

Mumford, Bart L (1985), "Cavitation Limits and the Effect of Aeration on Cone Valves".All Graduate Theses and Dissertations. 5079. https://digitalcommons.usu.edu/etd/5079

ISA (1995).RECOMMENDED PRACTICE Considerations for Evaluating Control

Valve Cavitation.In Consultant (Issue June).

Tullis, J. P., and Univ Colorado. 1976. “Testing Valves for Cavitation.” *Ci.Nii.Ac.Jp*. https://ci.nii.ac.jp/naid/10006921333/.

William J. Rahmeyer (1981) Journal (American Water Works Association), Vol. 73, No. 11, Sustaining Distribution Systems), pp. 582-585http://www.jstor.org/stable/41270610

Boffi, Pierpaolo, Giacomo Ferrarese, Maddalena Ferrario, Stefano Malavasi, Maria Vittoria Mastronardi, and Marco Mattarei. 2019. “Coherent Optical Fiber Interferometric Sensor for Incipient Cavitation Index Detection.” *Flow Measurement and Instrumentation* 66: 37–43. https://doi.org/10.1016/j.flowmeasinst.2018.11.005.

Ball, James W., J. Paul Tullis, and Travis Stripling. 1975. “PREDICTING CAVITATION IN SUDDEN ENLARGEMENTS.” *ASCE J Hydraul Div* 101 (7): 857–70. https://trid.trb.org/view/34426.

Knapp, R. T., Daily, J. W., and Hammitt, F. G. 1970, "Cavitation," McGraw-Hill BookCo., Inc., New York, NY, 578 pp.

Stripling, T. C. 1975, "Cavitation Damage Scale Effects: Sudden Enlargements," Thesispresented to Colorado State University, at Fort Collins, CO, in partial fulfillment of the requirements for the degree of Doctor of Philosophy, 135 pp.

Sweeney, C. E. 1974, "Cavitation Damage in Sudden Enlargements,"ThesispresentedtoColorado State University, at Fort Collins, CO, , in partial fulfillment of the requirementsfor the degree of Master of Science, 81 pp.

Ebrahimi, Behrouz, Guoliang He, Yingjie Tang, Matthew Franchek, Dong Liu, Jay Pickett, Frank Springett, and Dan Franklin. 2017. “Characterization of High-Pressure Cavitating Flow through a Thick Orifice Plate in a Pipe of Constant Cross Section.” *International Journal of Thermal Sciences* 114: 229–40. https://doi.org/10.1016/j.ijthermalsci.2017.01.001.

Baquero, F. 1977, "Cavitation Damage in Elbows," Thesis presented to Colorado State University, at Ft. Collins, CO., in partial fulfillment of the requirementsfor the degree of Master of Science.

Clyde, Eric S. 1977, "Cavitation Scale Effects in Pipe Elbows," Thesis presented to Colorado State University, at Fort Collins, CO., in partial fulfillment of the requirementsfor the degree of Master of Science.

Davis, Ted R. 1986, "Aerating Butterfly Valves To Suppress Cavitation," Thesis submitted to Utah State University, at Logan, Utah, , in partial fulfillment of the requirements for the degree of Master of Science.

Johnson, David. 1970. “Cavitation Parameters for Outlet Valves.” *Journal of the*

Hydraulics Division 96 (12): 2519–33. https://cedb.asce.org/CEDBsearch/record.jsp?dockey=0016859.

HAMMITT, F. G. 1973. “CAVITATION DAMAGE SCALE EFFECTS - STATE OF ART SUMMARIZATION.” Iahr.Tandfonline.Com, no. (AUGUST, 1973). https://iahr.tandfonline.com/doi/abs/10.1080/00221687509499717.

Carretero, J a, and Kenneth S Breuer. 2000. “Measurement and Modeling of the Flow Characteristics of Micro Disc Valves.” Microelectromechanical Systems, 1–8. https://www.researchgate.net/publication/251220374.

APPENDIX A

TECHNICAL DRAWINGS OF CAVITATION LATTICE

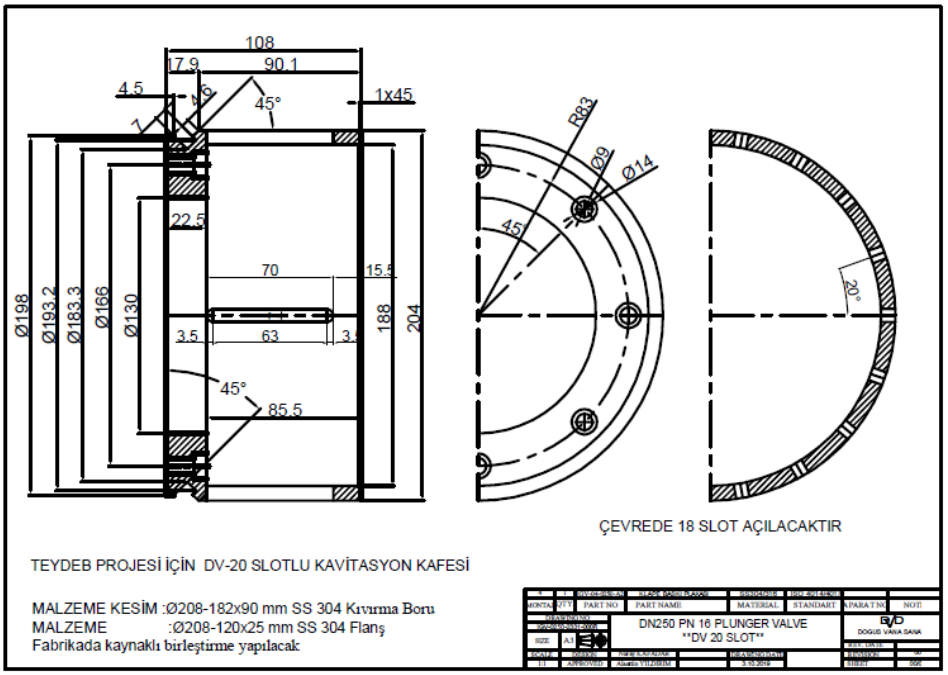

Figure A.1 Techical Drawing DV 20 Slot of DN 250 Plunger Valve

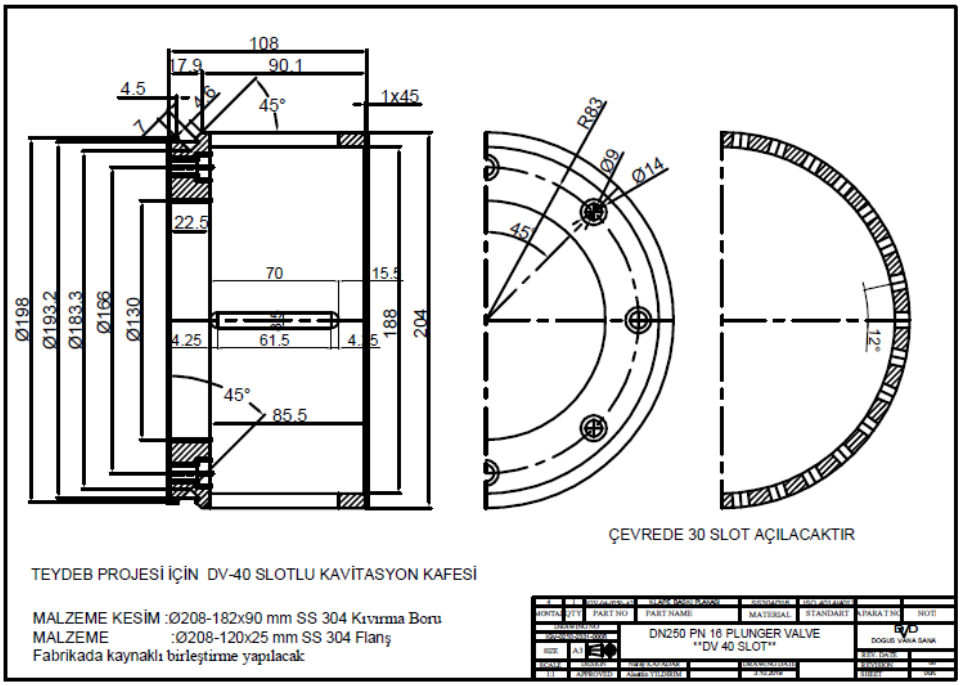

Figure A.2 Techical Drawing DV 40 Slot of DN 250 Plunger Valve

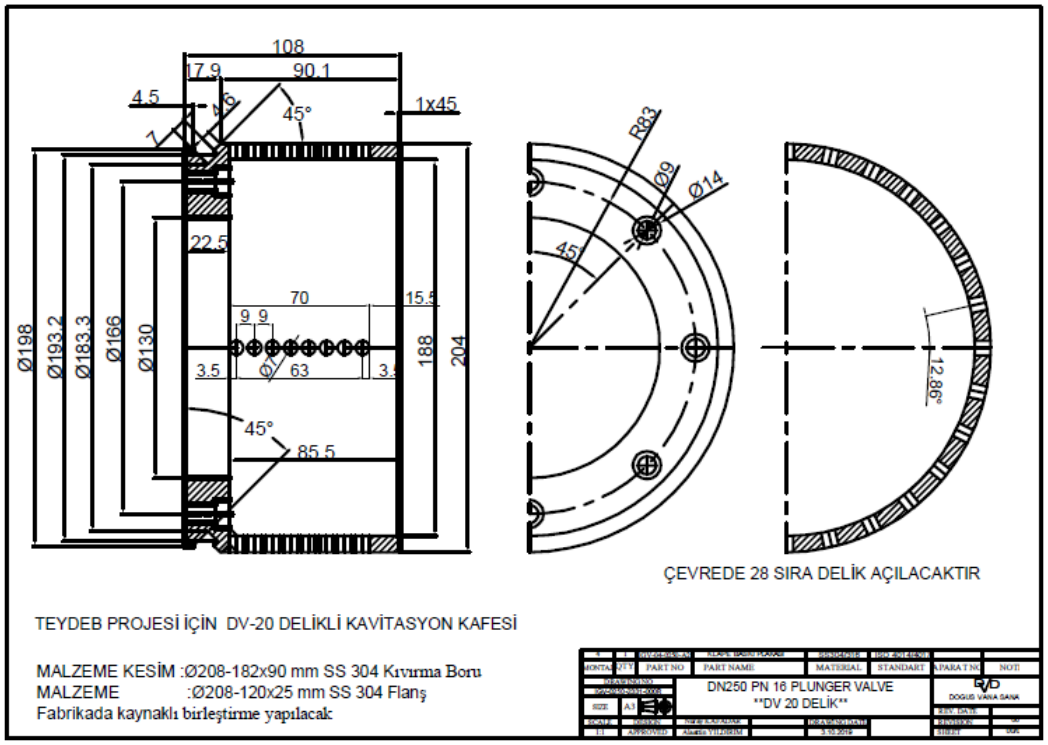

Figure A.3 Techical Drawing DV 20 Orifice of DN 250 Plunger Valve

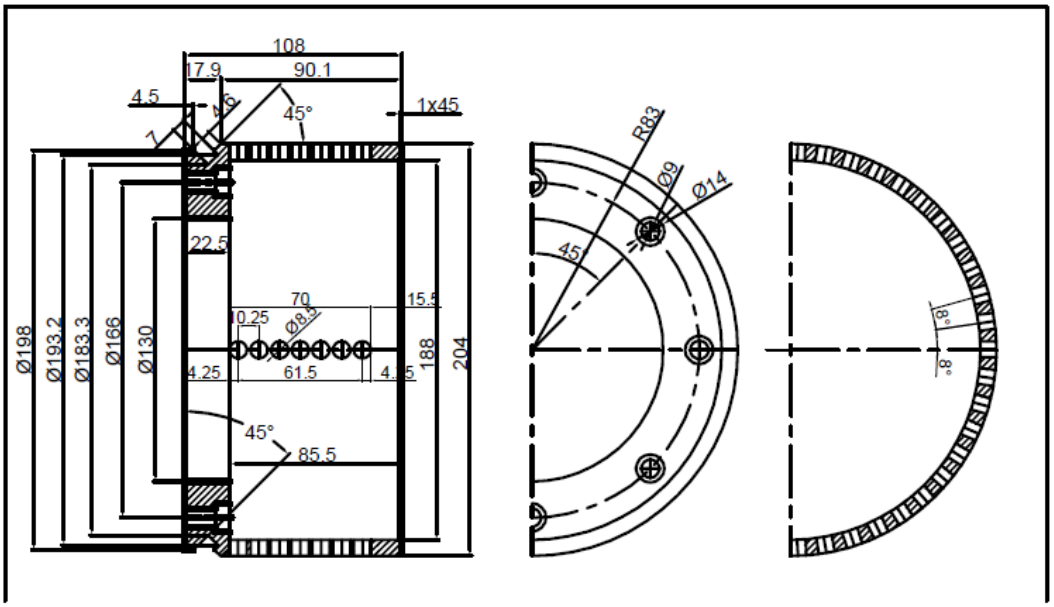

Figure A.4 Techical Drawing DV 40 Orifice of DN 250 Plunger Valve

APPENDIX B

TEST DEVICES AND DATA ACQUISITION SYSTEM

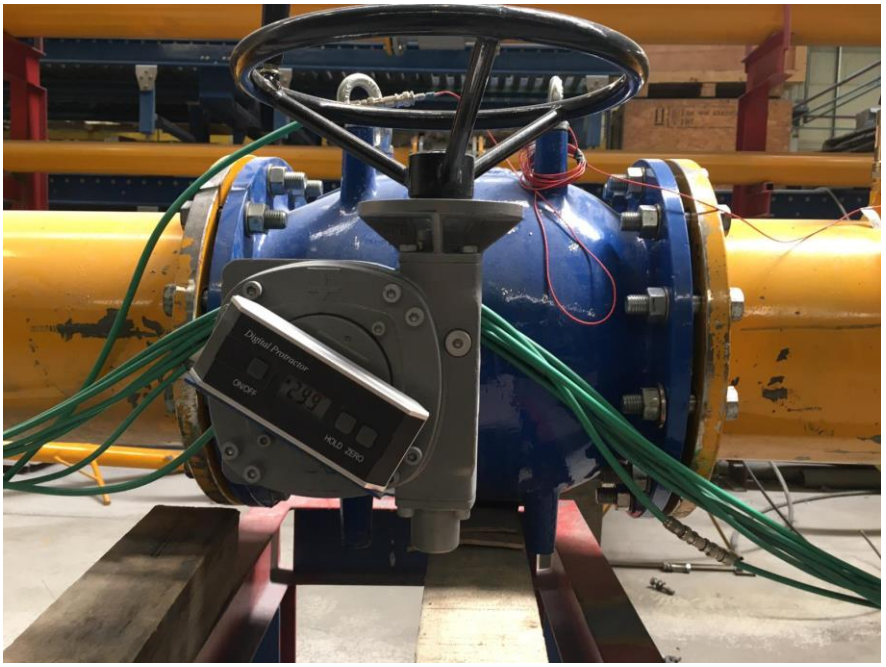

Figure B.1 Digital Protractor connected on Plunger Valve

Figure B.2 Pump Control Devices

Figure B.3 Centrifugal Pump

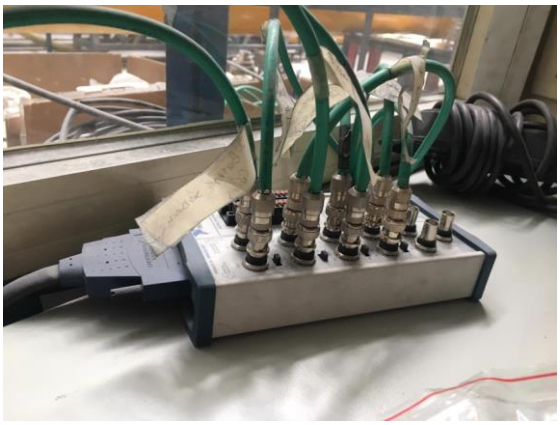

Figure B.4 NI USB-6341 BNC Terminal

Figure B.5 Accelerometer Preamplifier / NI PXIe – 1071 chassis / Power Supplies

APPENDIX C

CAVITATION TESTING SOFTWARE

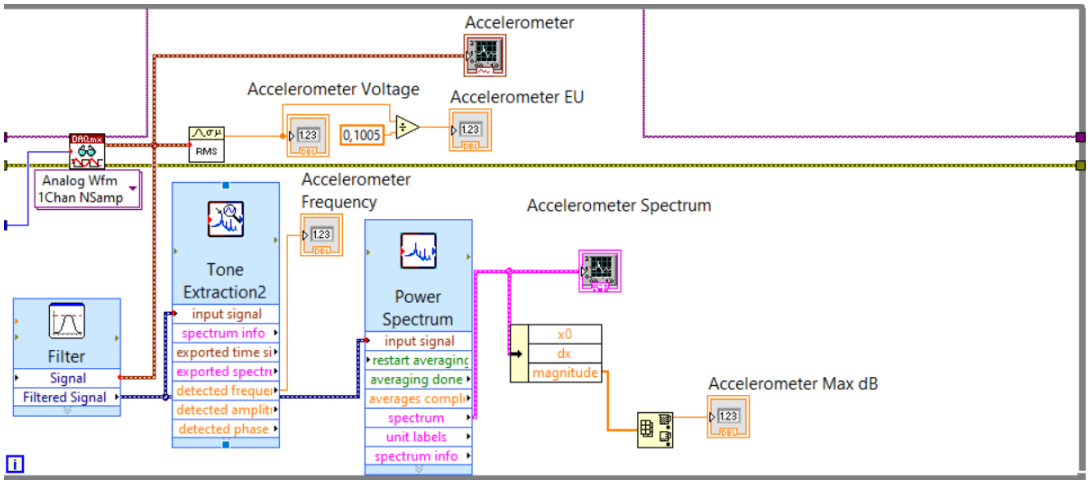

Figure C.1 Cavitation Detection Algorithm

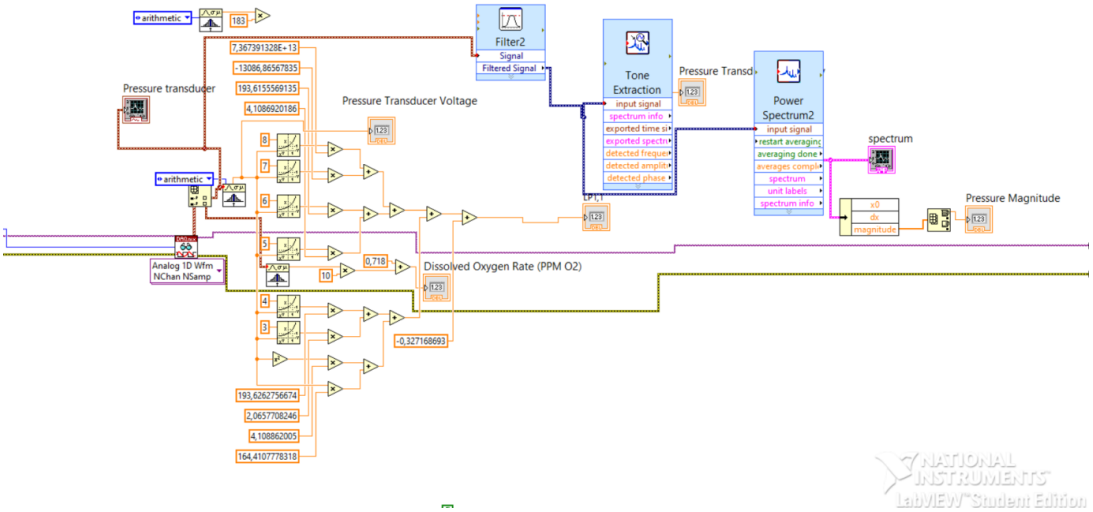

Figure C.2 Pressure Drop Performance Algorithm

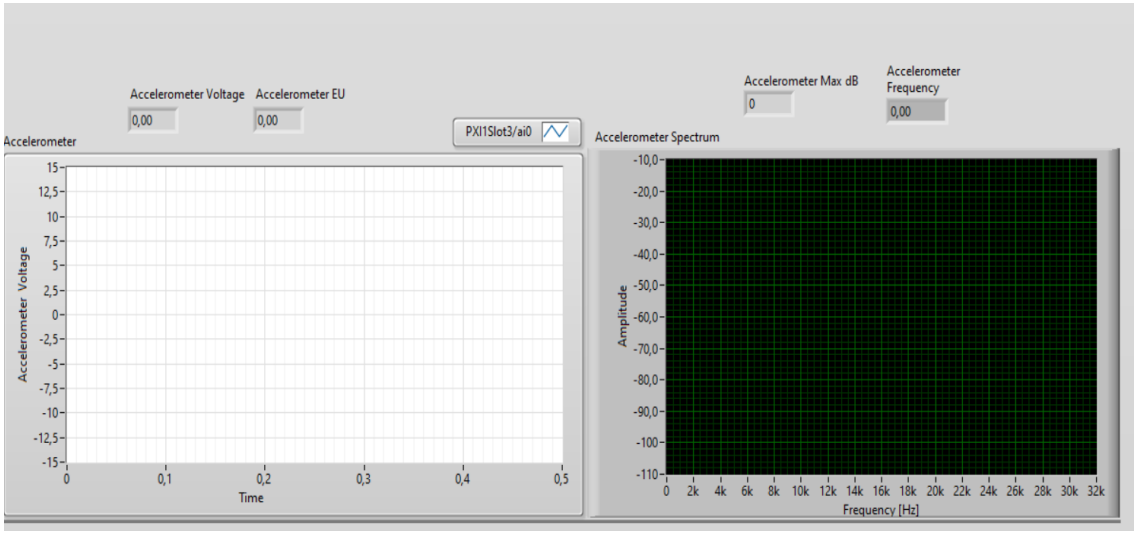

Figure C.3 Interface I

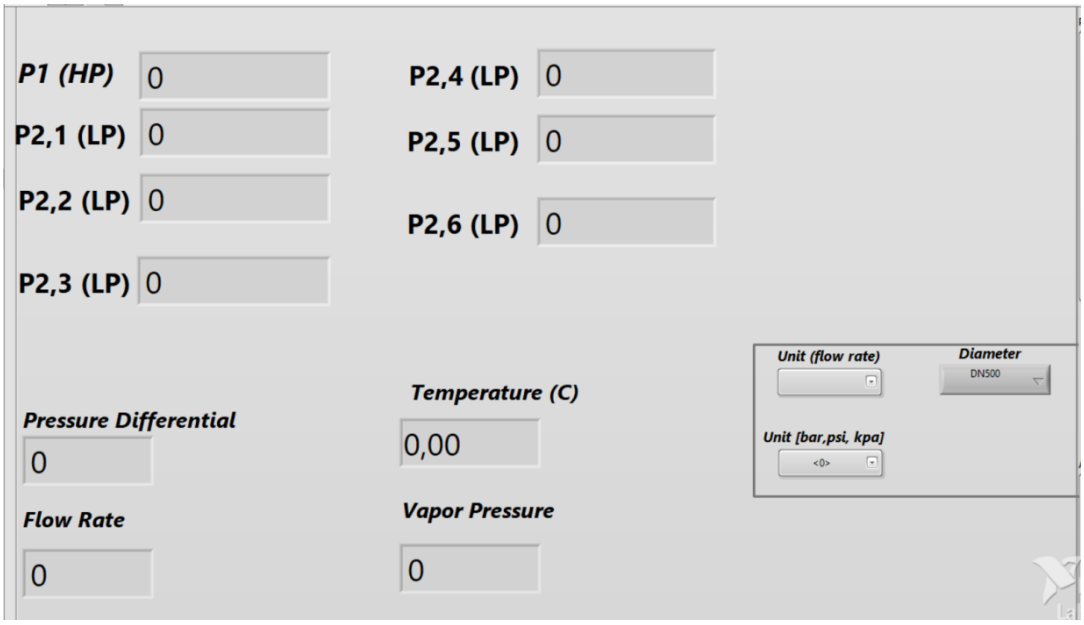

Figure C.3 Interface II

APPENDIX D

CAVITATION PARAMETER AND FLOW COEFFICEINT

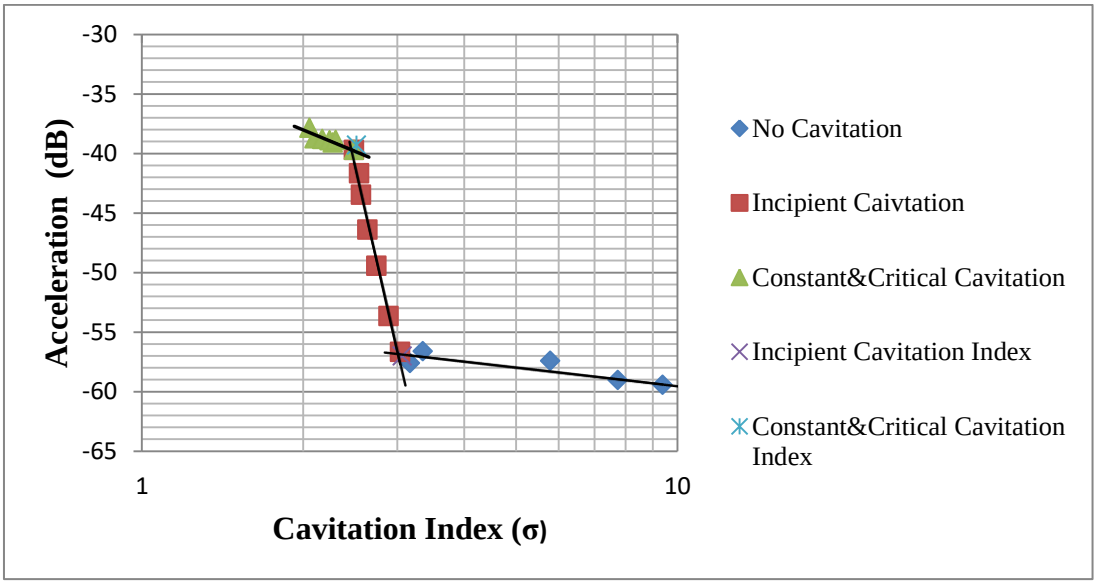

Figure D.1: Detecting Incipient and Critical Cavitation at 90˚ opening ratio for DN250 Plunger Valve DV20 Orifice

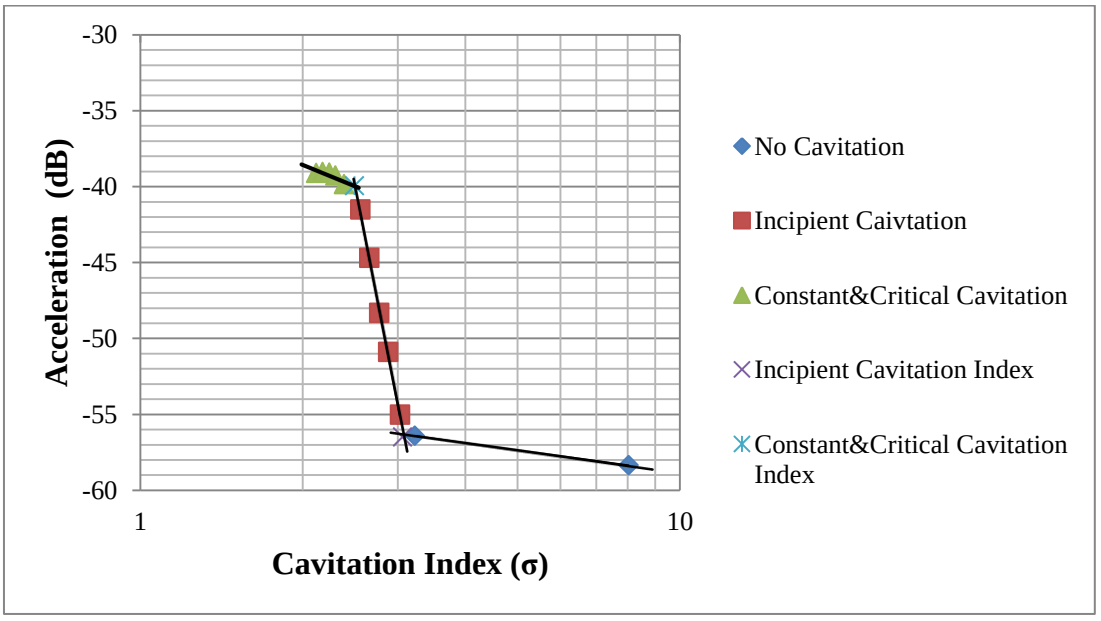

Figure D.2: Detecting Incipient and Critical Cavitation at 70˚ opening ratio for DN250 Plunger Valve DV20 Orifice

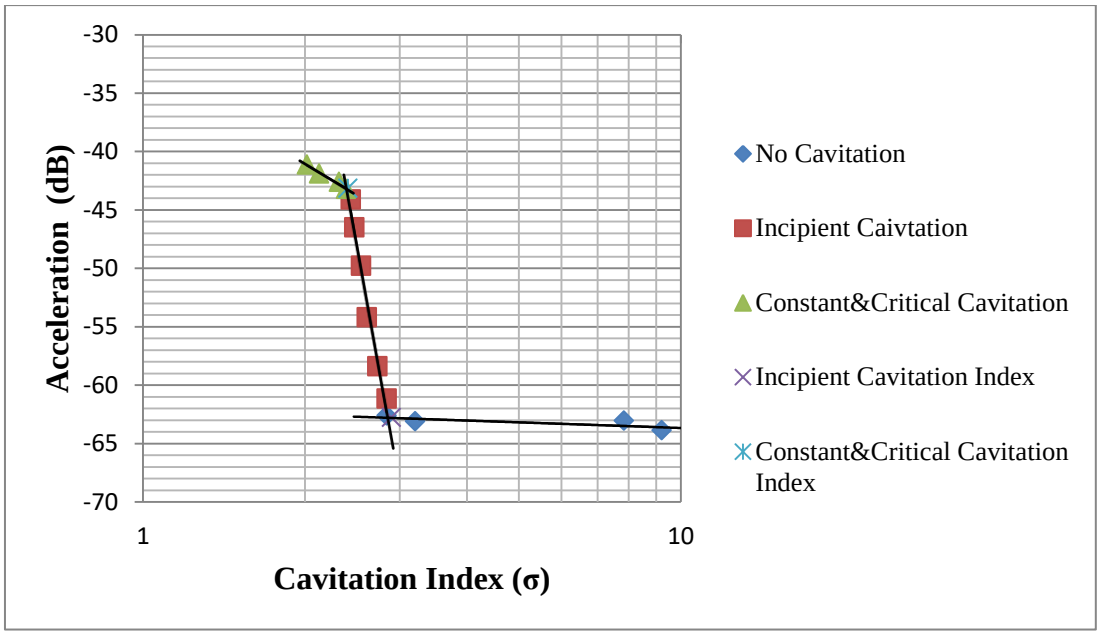

Figure D.3: Detecting Incipient and Critical Cavitation at 50° opening ratio for DN250 Plunger Valve DV20 Orifice

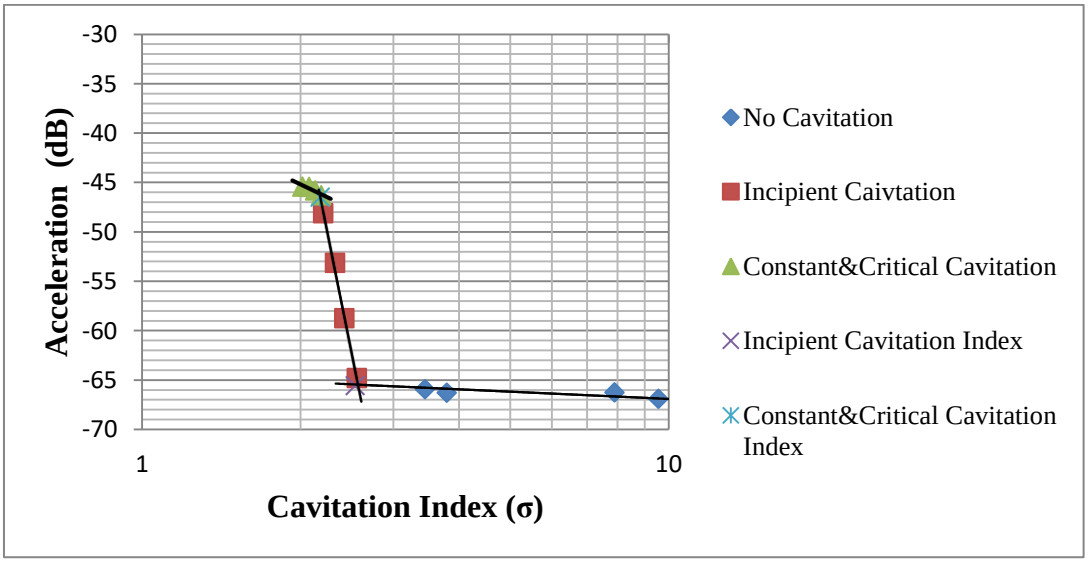

Figure D.4: Detecting Incipient and Critical Cavitation at 30° opening ratio for DN250 Plunger Valve DV20 Orifice

Table D.1 :Value of Cavitation Levels and Acceleration dB for DN 250 Plunger Valve (DV 20 Orifice)

Openings [°]	IncipientCavitation Index	Acceleration dB	Critical Cavitation Index	Acceleration dB
90	3,06	-57,01	2,51	-38,47
80	3,09	-54,61	2,50	-39,78
70	3,06	-56,49	2,49	-39,94
60	2,98	-58,50	2,42	-42,32
50	2,89	-62,78	2,40	-43,15
40	2,69	-65,50	2,32	-45,94
30	2,54	-65,58	2,18	-46,50
20	2,22	-65,58	2,03	-46,37

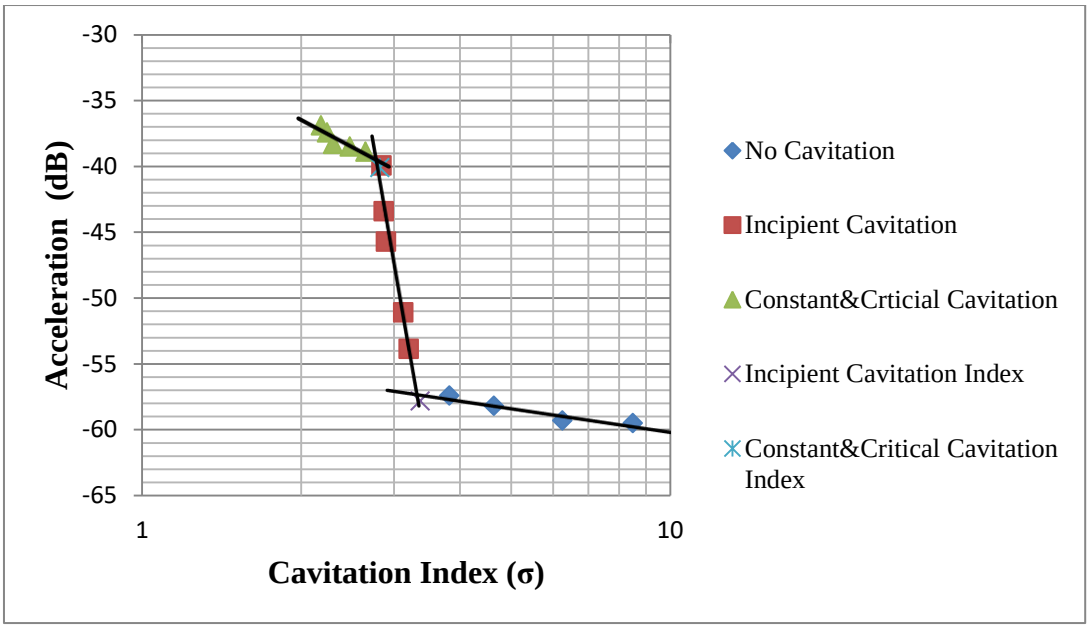

Figure D.5: Detecting Incipient and Critical Cavitation at 90° opening ratio for DN250 Plunger Valve DV20 Slot

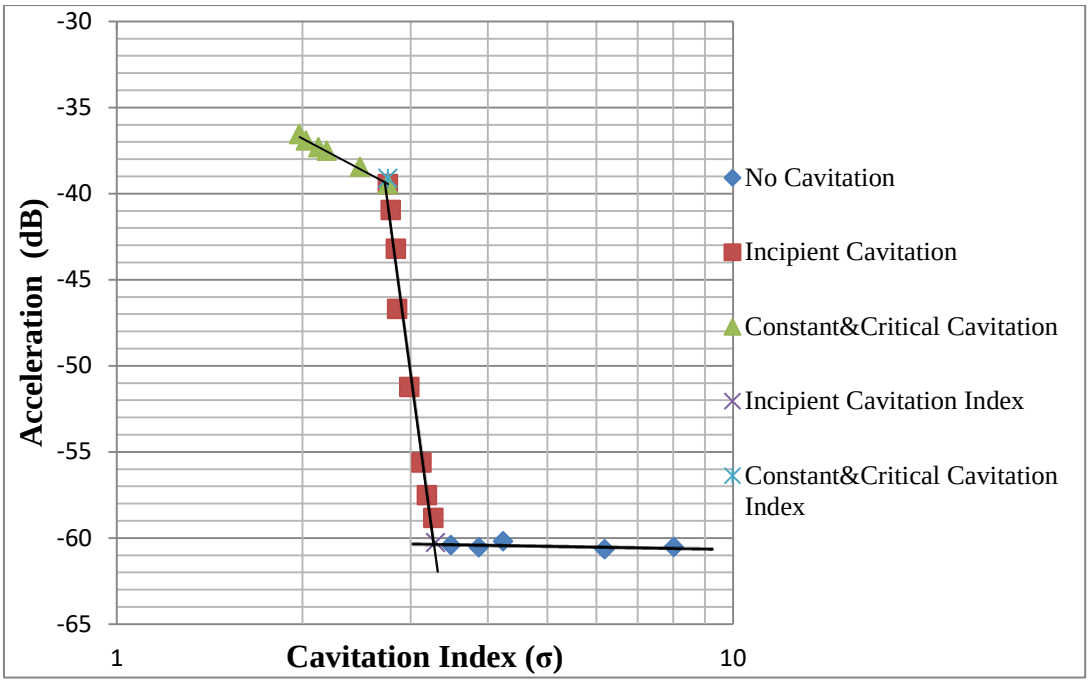

Figure D.6: Detecting Incipient and Critical Cavitation at 70° opening ratio for DN250 Plunger Valve DV20 Slot

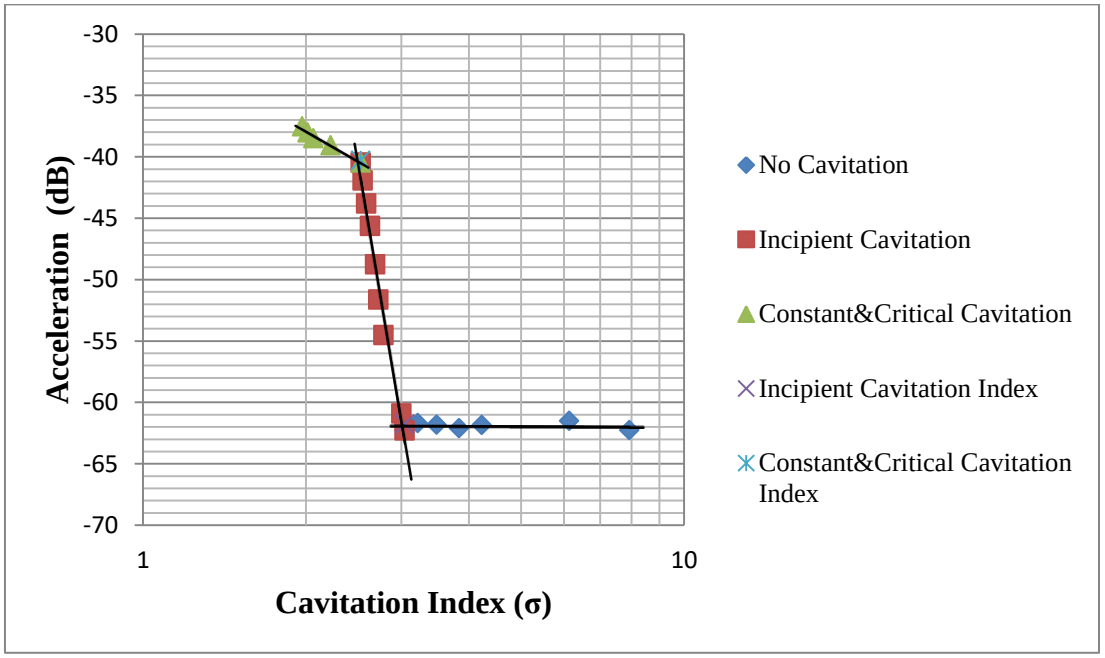

Figure D.7: Detecting Incipient and Critical Cavitation at 50° opening ratio for DN250 Plunger Valve DV20 Slot

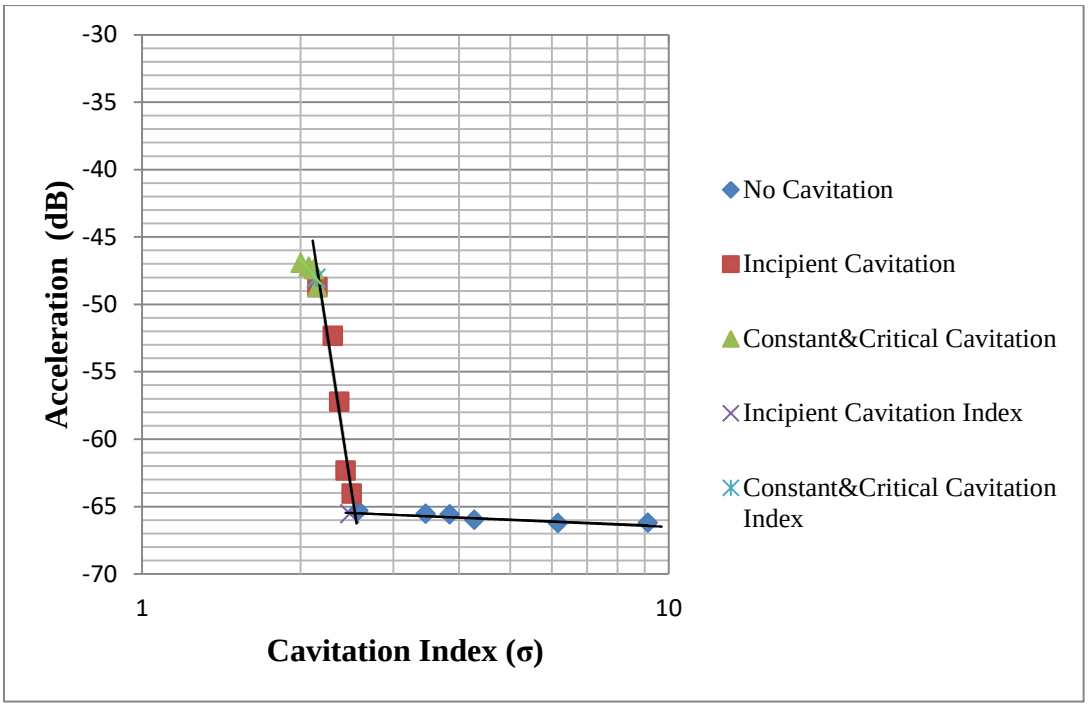

Figure D.8: Detecting Incipient and Critical Cavitation at 30° opening ratio for DN250 Plunger Valve DV20 Slot

Table D.2 :Value of Cavitation Levels and Acceleration dB for DN 250 Plunger Valve (DV 20 Slot)

Openings [°]	IncipientCavitation Index	Acceleration dB	Critical Cavitation Index	Acceleration dB
90	3,36	-57,84	2,82	-40,11
80	3,34	-57,06	2,81	-39,30
70	3,29	-58,26	2,75	-39,11
60	3,20	-61,30	2,66	-39,95
50	3,04	-61,76	2,25	-40,29
40	2,78	-64,07	2,32	-42,81
30	2,48	-65,54	2,14	-48,07
20	2,20	-71,34	2,00	-53,71

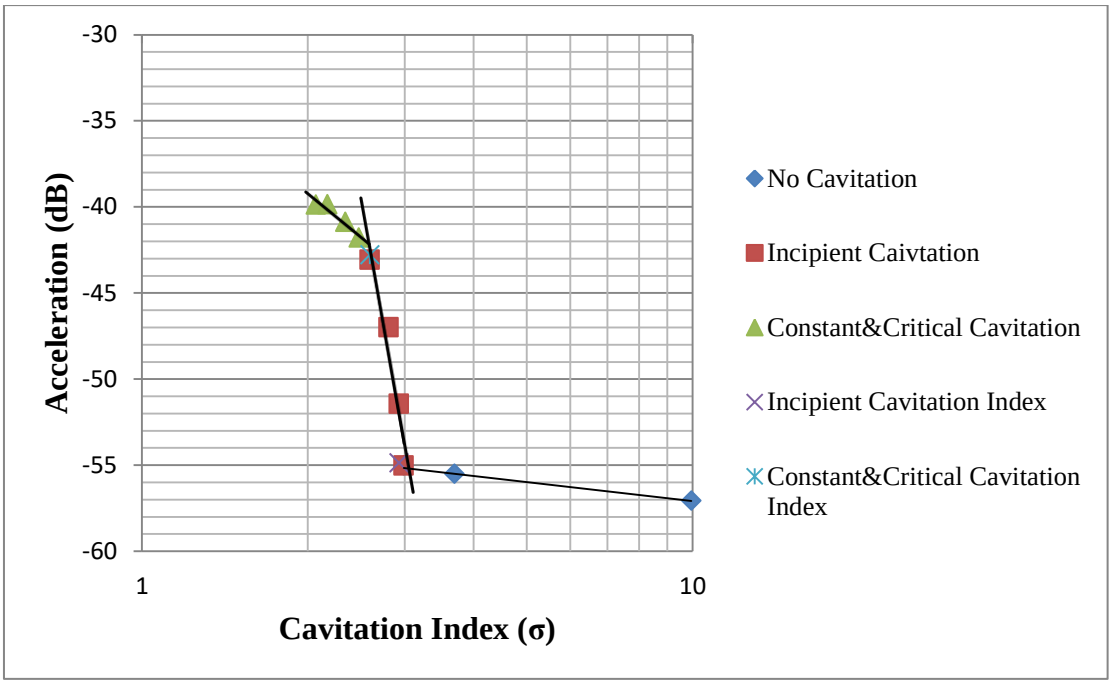

Figure D.9: Detecting Incipient and Critical Cavitation at 90° opening ratio for DN250 Plunger Valve DV40 Orifice

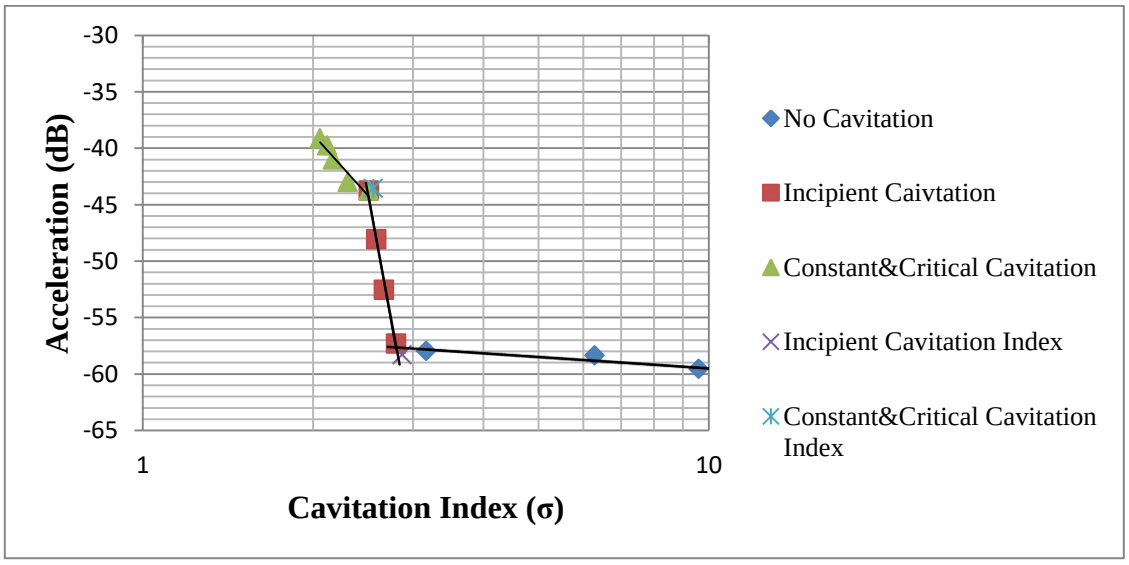

Figure D.10: Detecting Incipient and Critical Cavitation at 70° opening ratio for DN250 Plunger Valve DV40 Orifice

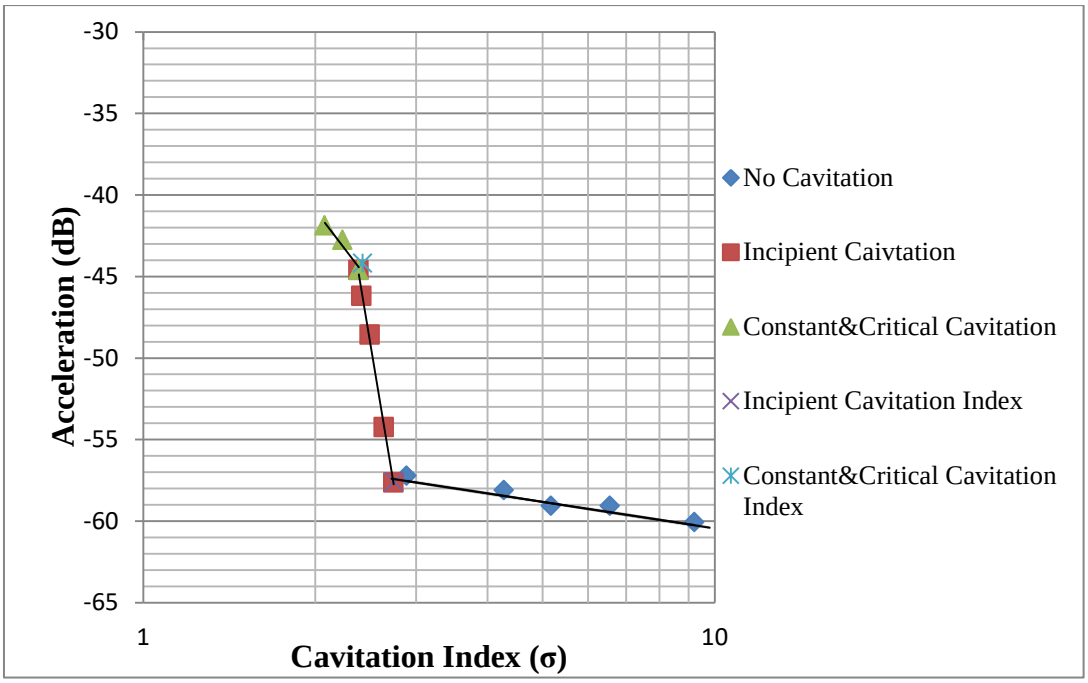

Figure D.11: Detecting Incipient and Critical Cavitation at 50° opening ratio for DN250 Plunger Valve DV40 Orifice

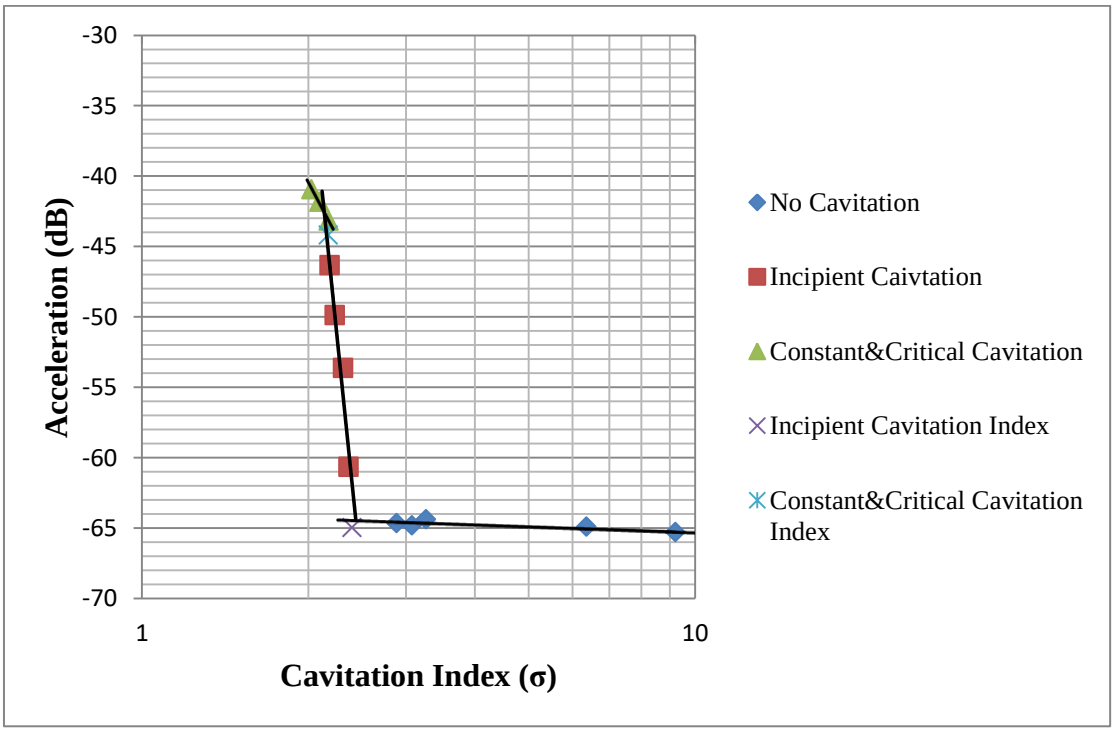

Figure D.12: Detecting Incipient and Critical Cavitation at 30° opening ratio for DN250 Plunger Valve DV40 Orifice

Table D.3 :Value of Cavitation Levels and Acceleration dB for DN 250 Plunger Valve (DV 40 Orifice)

Openings [°]	IncipientCavitation Index	Acceleration dB	Critical Cavitation Index	Acceleration dB
90	2,931	-54,878	2,593	-42,781
80	2,917	-60,238	2,589	-43,83
70	2,872	-58,28	2,554	-43,538
60	2,813	-55,95	2,462	-42,667
50	2,746	-57,616	2,419	-44,189
40	2,588	-61,549	2,31	-41,623
30	2,398	-64,967	2,172	-44,194
20	2,174	-66,193	2,008	-50,671

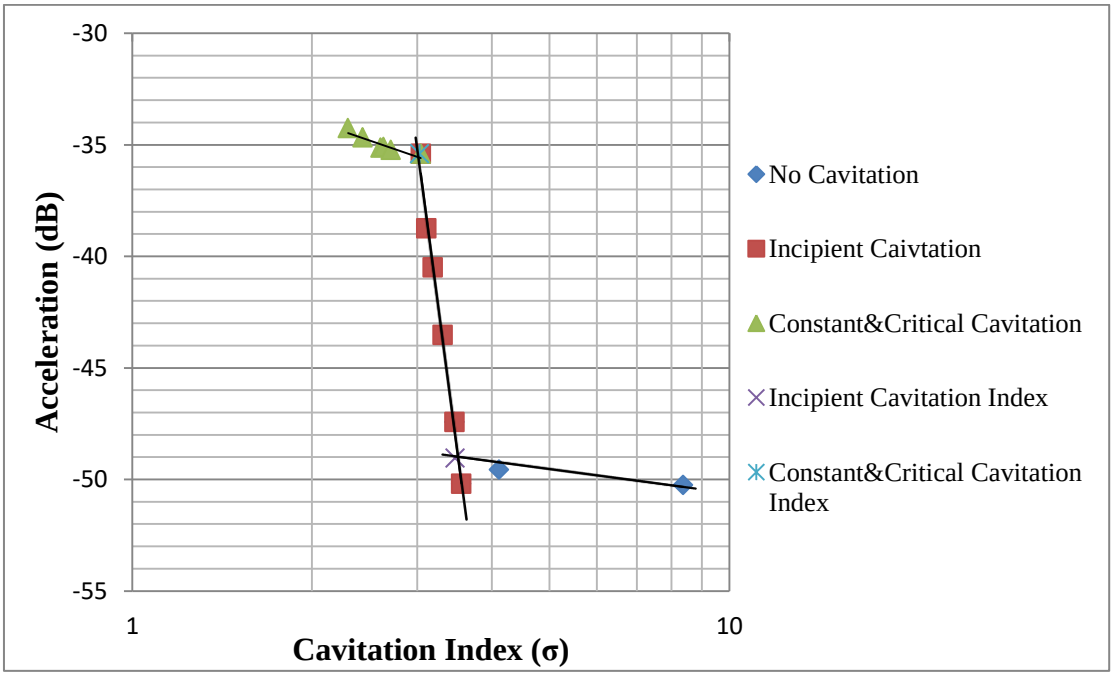

Figure D.13: Detecting Incipient and Critical Cavitation at 90° opening ratio for DN250 Plunger Valve DV40 Slot

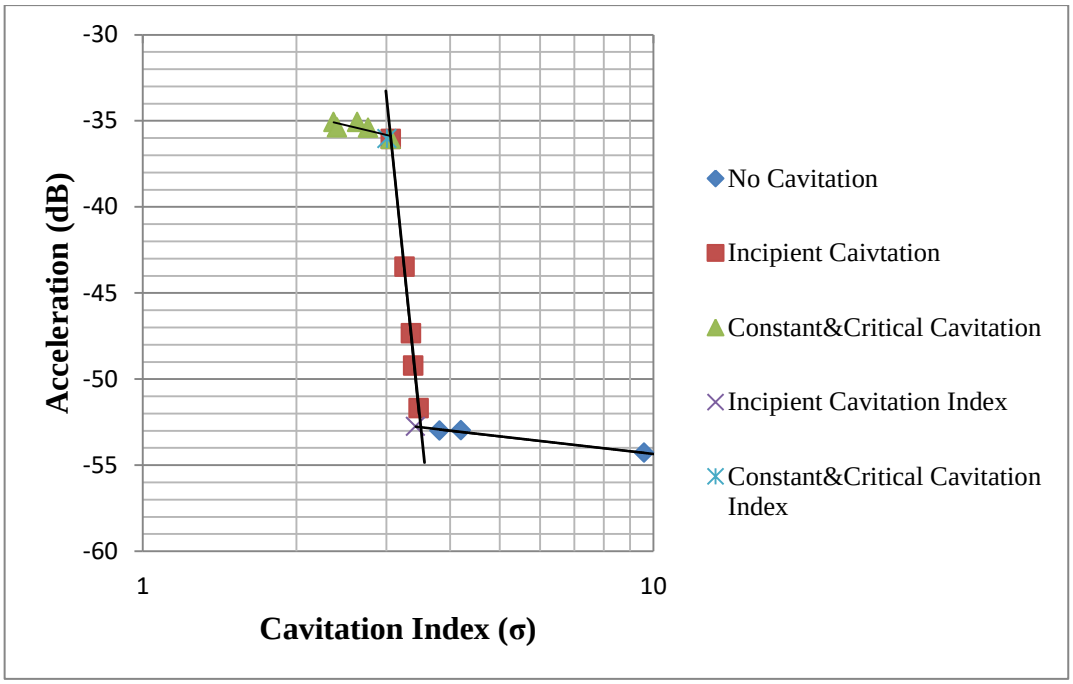

Figure D.14: Detecting Incipient and Critical Cavitation at 70° opening ratio for DN250 Plunger Valve DV40 Slot

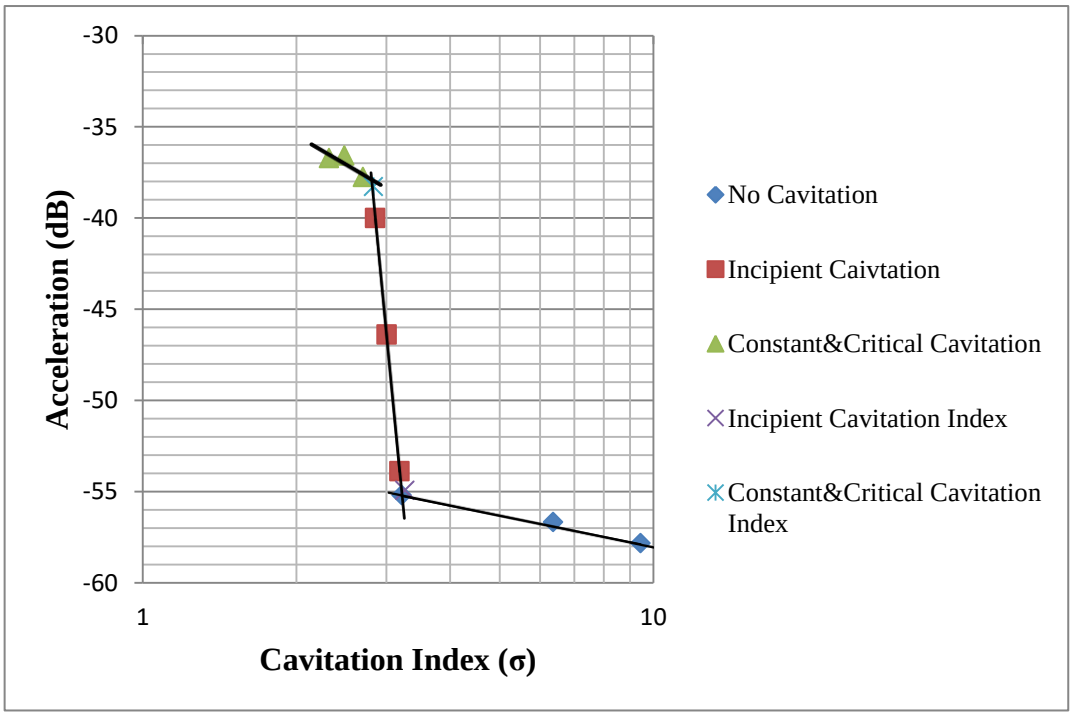

Figure D.15: Detecting Incipient and Critical Cavitation at 50° opening ratio for DN250 Plunger Valve DV40 Slot

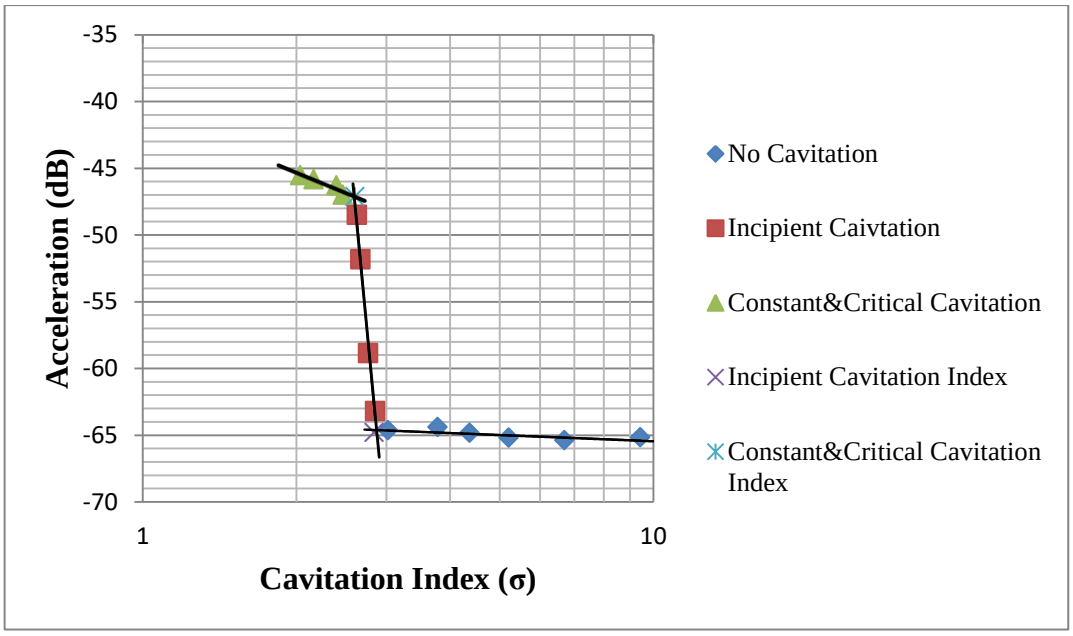

Figure D.16: Detecting Incipient and Critical Cavitation at 30˚ opening ratio for DN250 Plunger Valve DV40 Slot

Table D.4 :Value of Cavitation Levels and Acceleration dB for DN 250 Plunger Valve (DV 40 Slot)

Openings [°]	Incipient Cavitation Index	Acceleration dB	Critical Cavitation Index	Acceleration dB
90	3,471	-49,043	3,021	-35,404
80	3,523	-49,536	3,062	-36,509
70	3,423	-52,74	3,012	-36,041
60	3,314	-54,298	2,807	-37,663
50	3,261	-54,94	2,832	-38,289
40	3,113	-61,873	2,75	-42,839
30	2,841	-64,798	2,603	-47,143
20	2,581	-40,573	2,409	-58,06

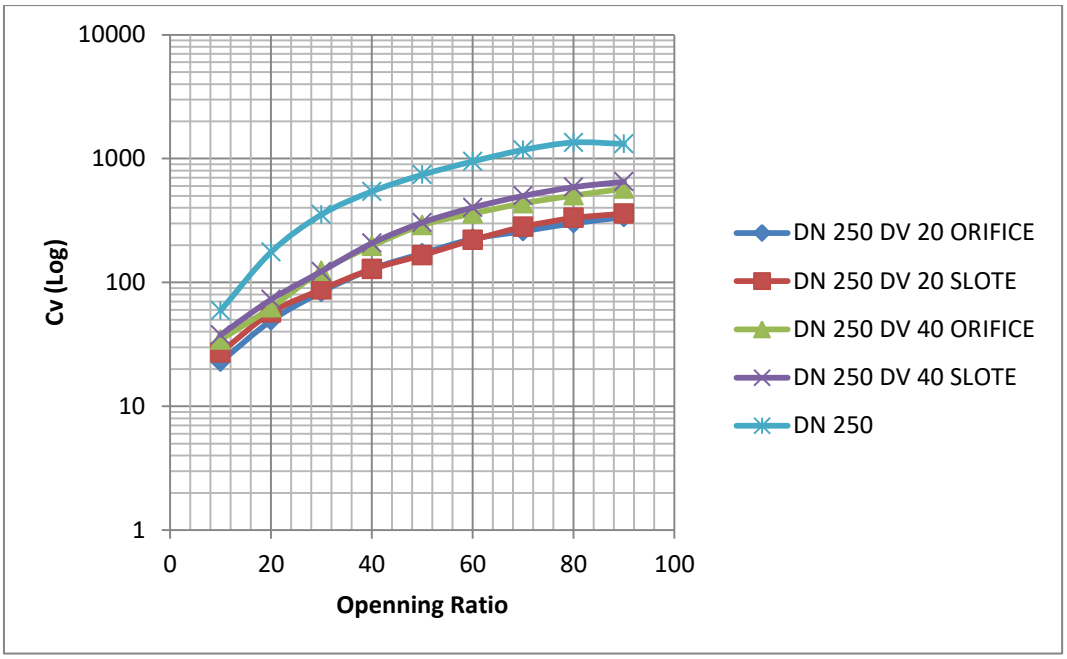

Figure D.17: Variation of Flow Coefficient with opening ratio for DN 250 Plunger Valve and Different Cavitation Lattice

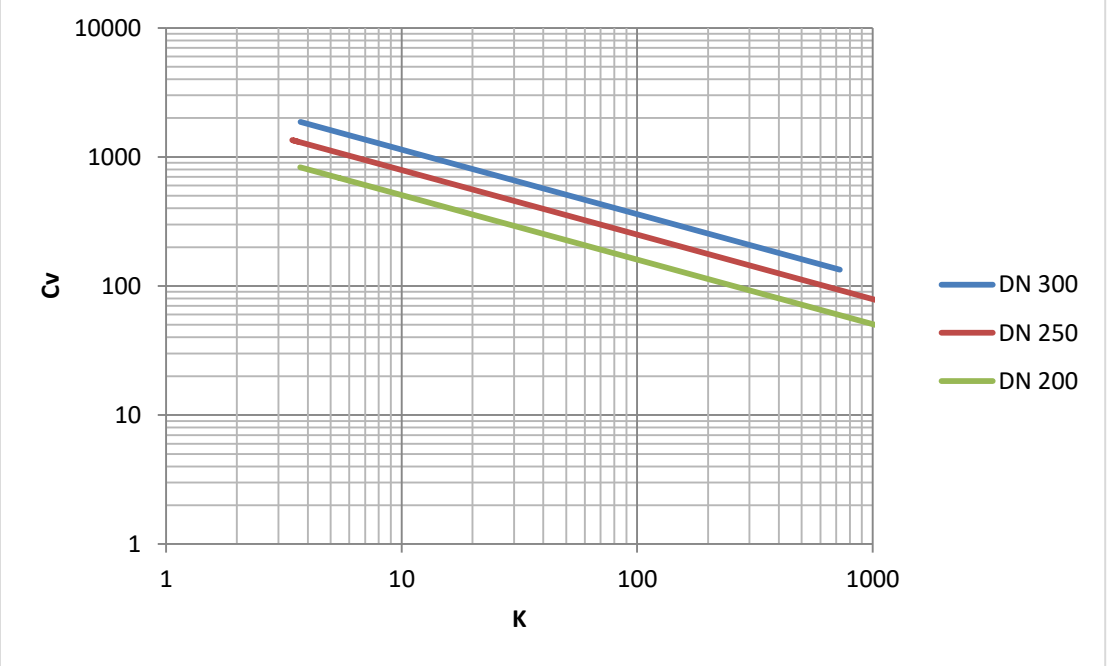

Figure D.18: Cv and K Conversion of Plunger Valves with Different Diameters.